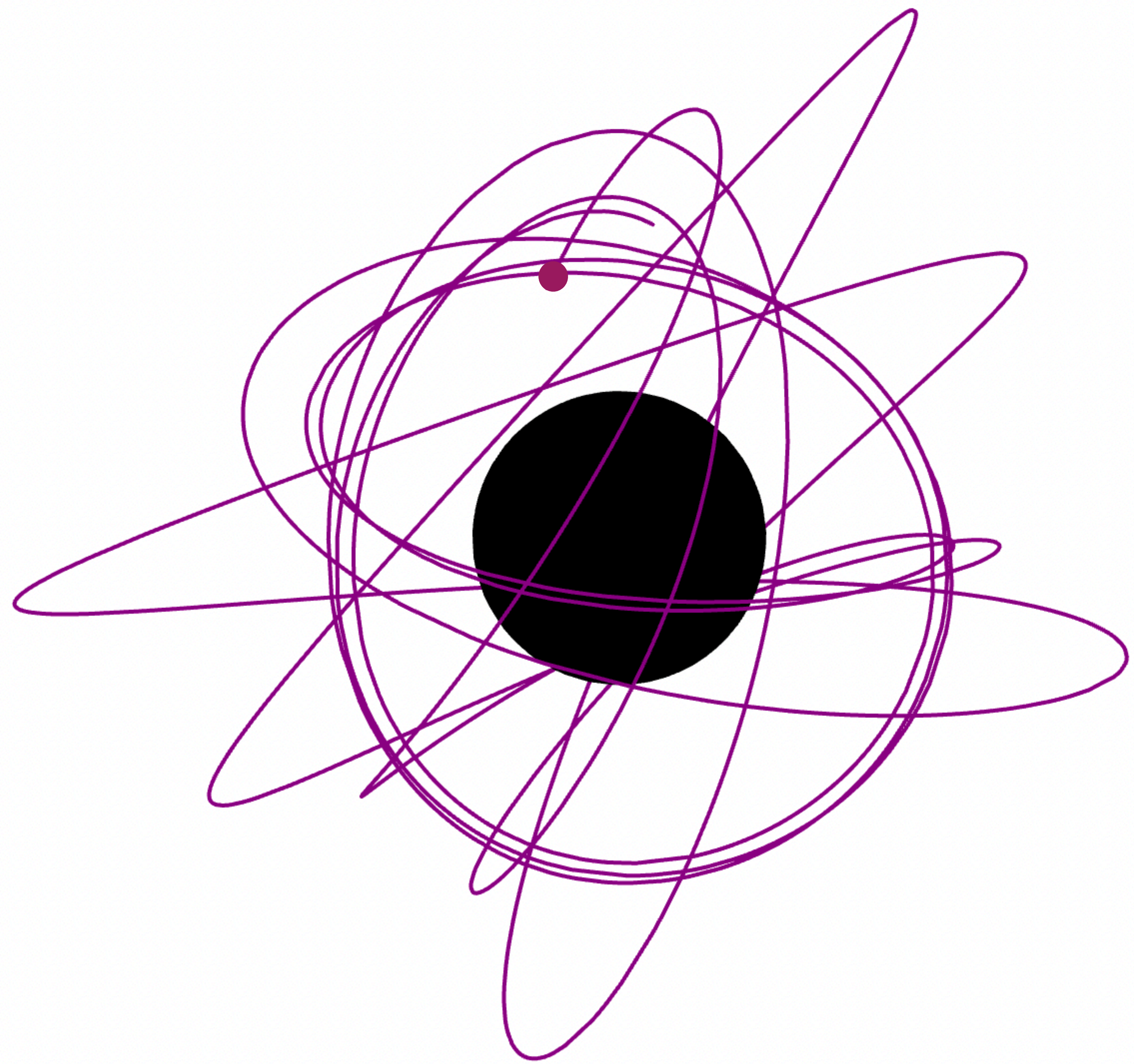

Modified EMRI Waveforms

Susanna Barsanti (She/her)
Postdoctoral Researcher @University College Dublin

The framework

❋Theory agnostic approach: shift-symmetric theories with a new massless scalar field

- *generalised scalar-tensor theories*
- *scalar Gauss-Bonnet*
- *dynamical Chern Simons*
- *f(R) theories ...*

$$S\left[\mathbf{g},\varphi,\Psi\right] = S_0\left[\mathbf{g},\varphi\right] + \alpha S_c\left[\mathbf{g},\varphi\right] + S_m\left[\mathbf{g},\varphi,\Psi\right]$$

$$\int d^4x \frac{\sqrt{-g}}{16\pi}\left(R - \frac{1}{2}\partial_\mu\varphi\partial^\mu\varphi\right)$$

Non minimal coupling

matter fields Ψ

❋Single expansion parameter: mass ratio q $\begin{cases} g_{\mu\nu} = g^{(0)}_{\mu\nu} + q h^{(1)}_{\mu\nu} + \mathcal{O}(q^2) \\ \varphi = \varphi^{(0)} + q\varphi^{(1)} + \mathcal{O}(q^2) \end{cases}$

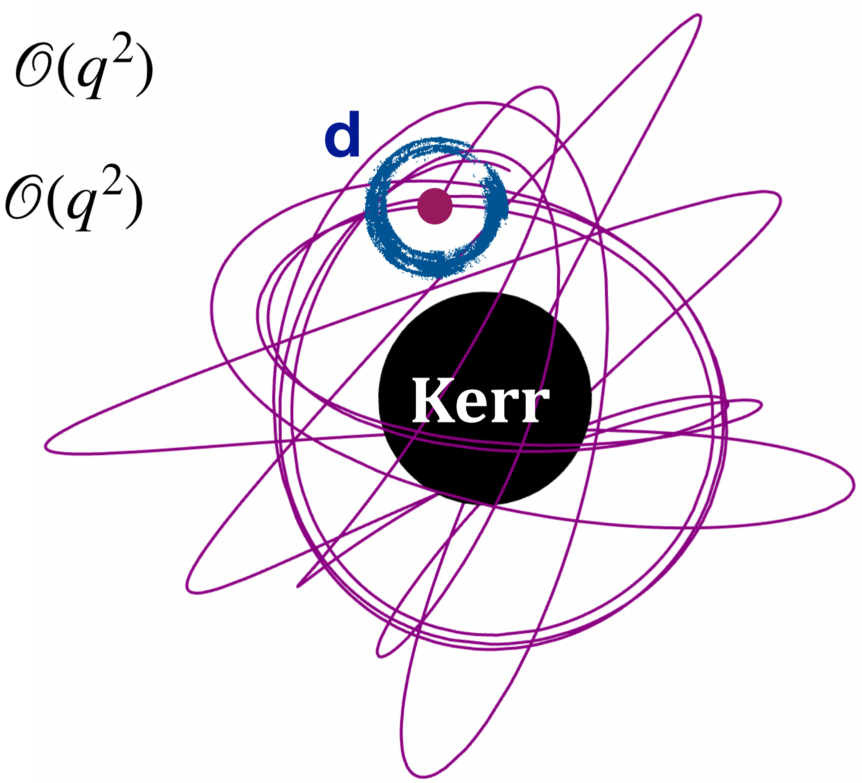

- First order:

$$G^{(1)}_{\mu\nu} = 8\pi m_p \int \frac{\delta^{(4)}(x - y_p(\lambda))}{\sqrt{-g}} \frac{dy^p_\mu}{d\lambda} \frac{dy^p_\nu}{d\lambda} d\lambda$$

$$\Box\varphi^{(1)} = -4\pi\, d\, m_p \int \frac{\delta^{(4)}(x - y_p(\lambda))}{\sqrt{-g}} d\lambda$$

Solved with the Teukolsky approach: $\psi^{(s)}(t,r,\theta,\phi) = \int d\omega \sum_{\ell m} R^{(s)}_{\ell m}(r,\omega) S^{(s)}_{\ell m}(\theta,\omega) e^{im\phi} e^{-i\omega t}$

- Second order: $a = a_{(1)grav} + a_{(1)scal} + a_{(2)grav} + a_{(2)scal}$

The research project: mindset & literature

- EMRIs + scalar fields: *A. Maselli+, Phys.Rev.Lett.* 125 (2020) 14, 141101

➡ **Post-adiabatic terms**

- Formalism: *A. Spiers+, Phys.Rev.D 109 (2024) 6, 064022*
- Implementation: In progress…

➡ **Orbits**

- Equatorial eccentric around Kerr: *S.B+, Phys.Rev.D 106 (2022) 4, 044029*
- Circular inclined around Kerr : *M. Della Rocca+, Phys.Rev.D 109 (2024) 10, 104079*
- Generic (eccentric&inclined): In progress… *S. Gliorio+*

➡ **Parameter estimation**

- Fisher Information Matrix: *A. Maselli+, Nature Astron. 6 (2022) 4, 464-470*
- Markov Chain Monte Carlo: *L. Speri+, ArXiv2406.07607*

➡ **Non shift-symmetric fields**

- Massive scalar fields: *S.B+, Phys.Rev.Lett. 131 (2023) 5, 051401*

0PA

Modeling Steps

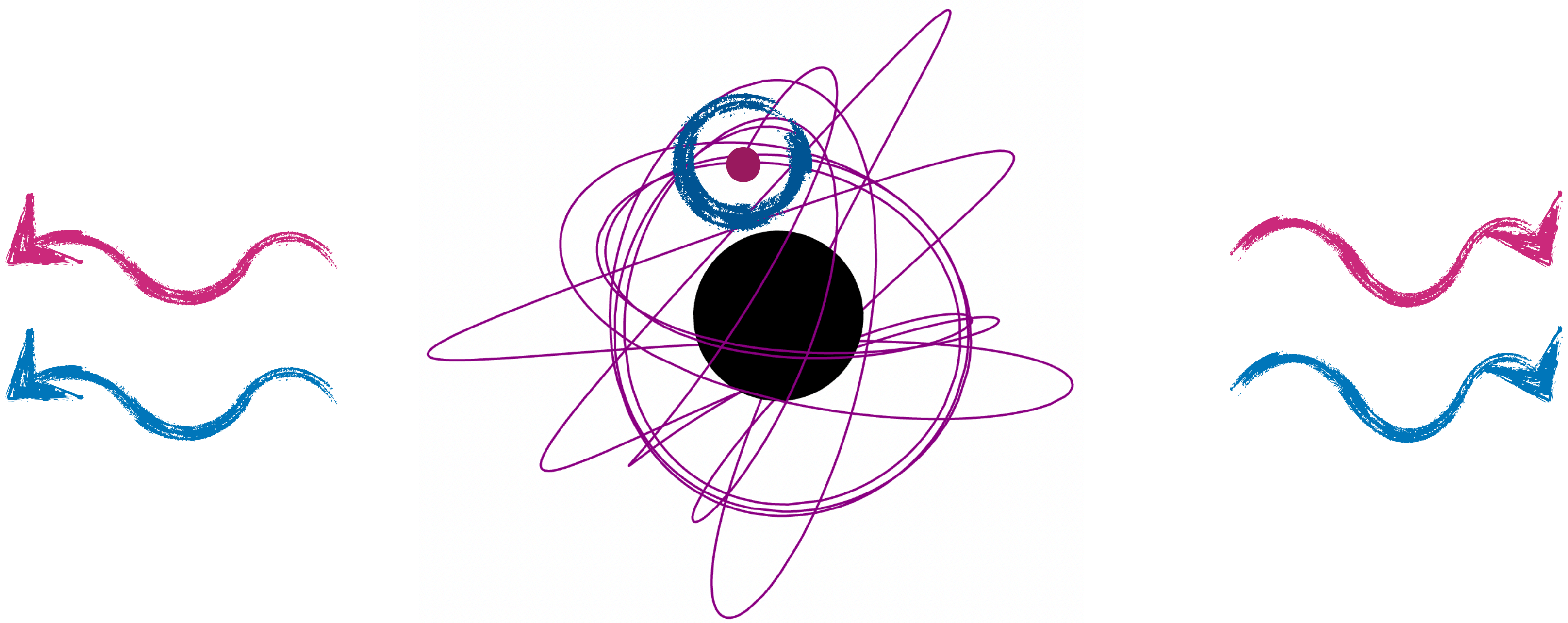

- *Energy emission trough gravitational and scalar waves*

$$\dot{E}_W = \sum_{i=+,-} [\dot{E}^{(i)}_{\rm grav} + \dot{E}^{(i)}_{\rm scal}] = \dot{E}_{grav} + \dot{E}_{scal} \longrightarrow \dot{E}_{scal} \propto d^2$$

EXTRA emission *simply added* to the gravitational one!

- *Adiabatic orbital evolution through a sequence of geodesics*
- *Imprint on the gravitational waves: dephasing, faithfulness*
- *Parameter estimation: FIM, MCMC*

GW template: Analytical Kludge

- Quadrupolar approximation $$h_{ij}^{TT} = \frac{2}{D}\left(P_{i\ell}P_{jm} - \frac{1}{2}P_{ij}P_{\ell m}\right)\ddot{I}_{\ell m}$$

[L. Barack and C. Cutler, Phys. Rev. D 69 (2004) 082005]

$$I_{ij} = \int d^3x T^{tt}(t, x^i)x^i x^j = m_p x^i x^j$$

- Strain measured by the detector $$h(t) = \sum_n h_n(t) \qquad h_n(t) = \frac{\sqrt{3}}{2}\left[F^+(t)A_n^+(t) + F^\times(t)A_n^\times(t)\right]$$

LISA pattern functions

$$F_+ = \frac{1+\cos^2\theta}{2}\cos 2\phi \cos 2\psi - \cos\theta \sin 2\phi \sin 2\psi$$
$$F_\times = \frac{1+\cos^2\theta}{2}\cos 2\phi \sin 2\psi + \cos\theta \sin 2\phi \cos 2\psi$$

Amplitudes

$$A_n^+ = -[1+(\hat{L}\cdot\hat{N})^2][a_n\cos(2\gamma) - b_n\sin(2\gamma)] + [1-(\hat{L}\cdot\hat{N})^2]c_n$$
$$A_n^\times = 2(\hat{L}\cdot\hat{N})[b_n\cos(2\gamma) + a_n\sin(2\gamma)]$$

$$a_n = -n\boxed{\mathscr{A}}\left[J_{n-2}(ne) - 2eJ_{n-1}(ne) + (2/n)J_n(ne) + 2eJ_{n+1}(ne) - J_{n+2}(ne)\right]\cos[n\Phi(t)]$$

$$b_n = -n\boxed{\mathscr{A}}(1-e^2)^{1/2}[J_{n-2}(ne) - 2J_n(ne) + J_{n+2}(ne)]\sin[n\Phi(t)]$$

$$c_n = 2\boxed{\mathscr{A}}J_n(ne)\ \cos[n\Phi(t)]$$

$$\mathscr{A} \rightarrow (2\pi\nu M)^{2/3}m_p/D$$

$$\begin{cases} 2\pi\nu = d\Phi/dt \\ \Phi = \Psi_\phi \\ \cos\gamma = \cos\Psi_R \end{cases}$$

Faithfulness: Equatorial ECCENTRIC EMRIs

Estimate of how much two signals differ: $\mathcal{F}[h_1, h_2] = \max_{\{t_c, \phi_c\}} \frac{\langle h_1 | h_2 \rangle}{\sqrt{\langle h_1 | h_1 \rangle \langle h_2 | h_2 \rangle}}$

Inner product $\langle h_1 | h_2 \rangle = 4\Re \int_{f_{min}}^{f_{max}} \frac{\tilde{h}_1(f)\tilde{h}_2^\star(f)}{S_n(f)} df$

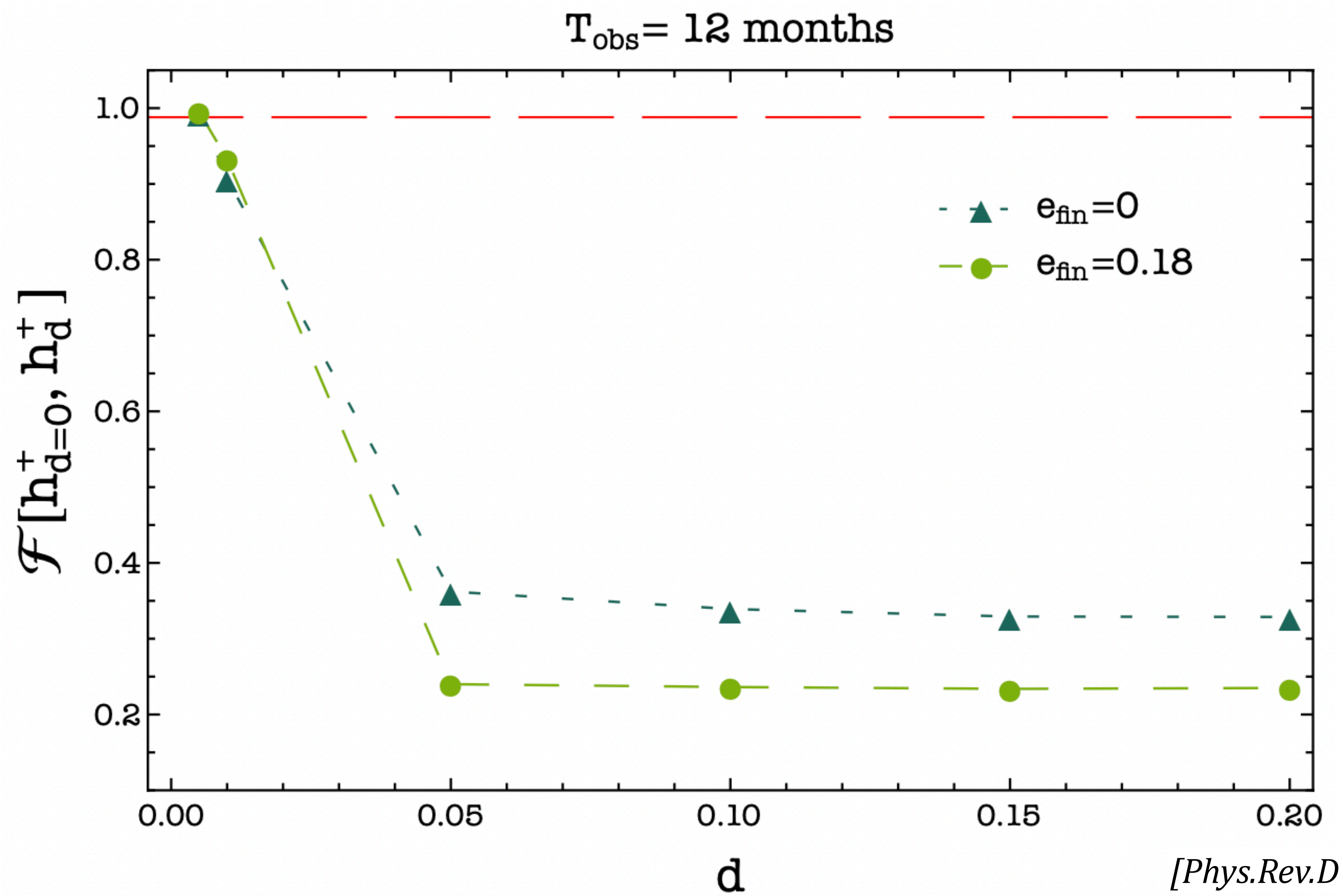

detectable effect !

[Phys.Rev.D 106 (2022) 4, 044029]

- Red line: threshold under which the signals are significantly different - $\mathcal{F} \lesssim 0.994$ for $SNR = 30$
- After 1year $\mathcal{F}$ is always smaller than the threshold for scalar charges as small as $d = 0.01$
- For the eccentric inspirals the distinguishability increases

Faithfulness: INCLINED Circular EMRIs

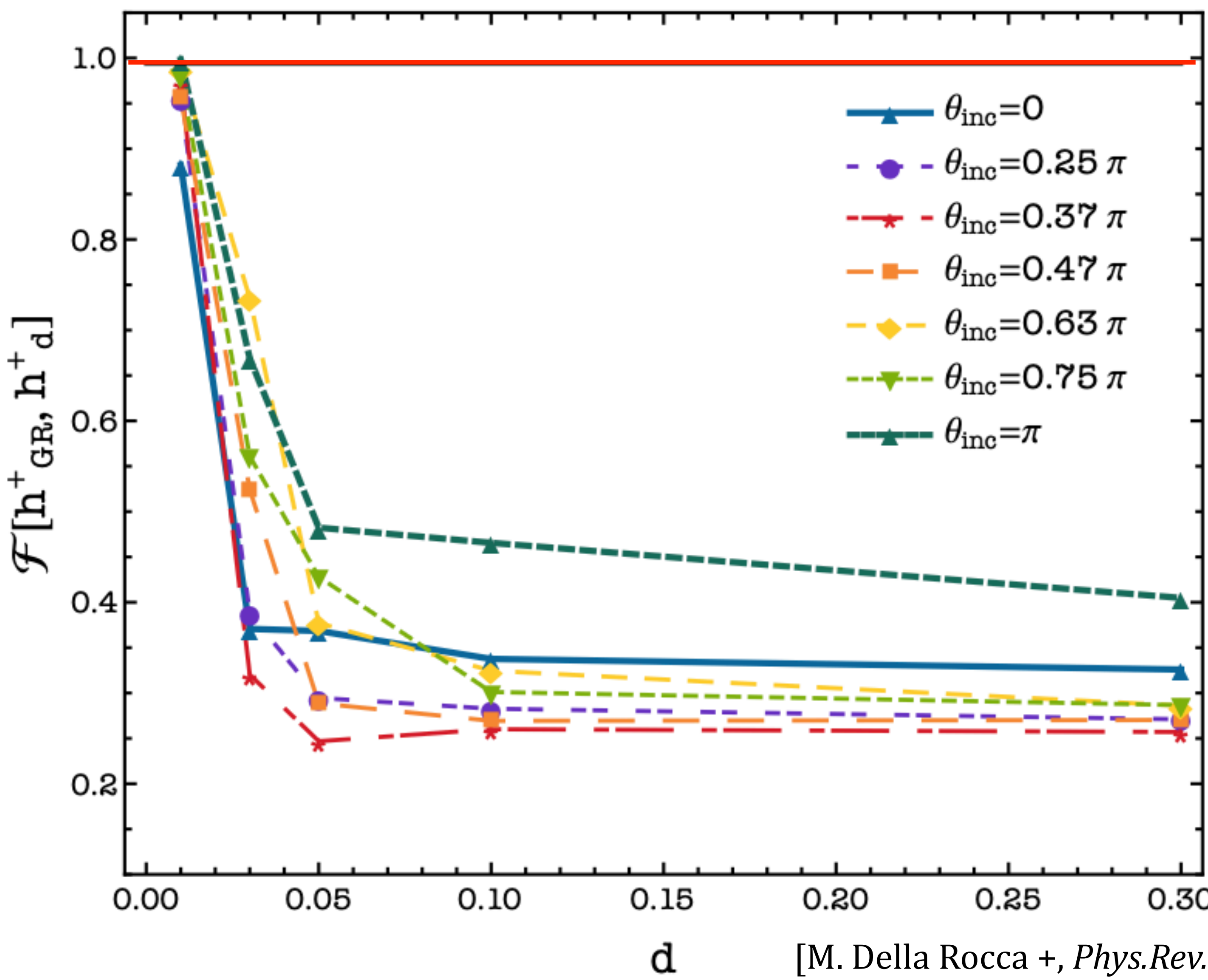

[M. Della Rocca +, *Phys.Rev.D 109 (2024) 10, 104079*]

- Red line: threshold under which the signals are significantly different - $\boxed{\mathscr{F} \lesssim 0.994 \text{ for } SNR = 30}$
- After 1year $\mathscr{F}$ is always smaller than the threshold for scalar charges as small as $d \simeq 0.05$
- The mismatch increases with the increasing of the orbital inclination, for prograde orbits

Bayesian Analysis

- Bayes' theorem

$$\underbrace{p(\boldsymbol{\theta}|d)}_{\text{Posterior}} = \frac{\overbrace{p(d|\boldsymbol{\theta})}^{\text{Likelihood}}\,\overbrace{p(\boldsymbol{\theta})}^{\text{Priors}}}{p(d)}$$

- Stochastic sampling technique: Markov Chain Monte Carlo (MCMC)

- 13 waveform parameters: $\vec{\theta} = \left(\ln M, \ln m_p, \frac{a}{M}, \ln D, \theta_S, \phi_S, \theta_L, \phi_L, p_0, e_0, \Phi_{\phi 0}, \phi_{r0}, d\right)$

LISA pipeline **F**ast **E**MRI **W**aveforms

0PA	Circular	Eccentric	Generic
Schwarzschild	Fully Relativistic (also 1PA!)	Fully Relativistic	AAK
Kerr	AAK	AAK	AAK

Bayesian Analysis: Results

FastEMRIWaveforms: fully relativistic equatorial **eccentric** inspiral, **AAK** waveforms

Injected GR ($d = 0$), recovered $d \neq 0$

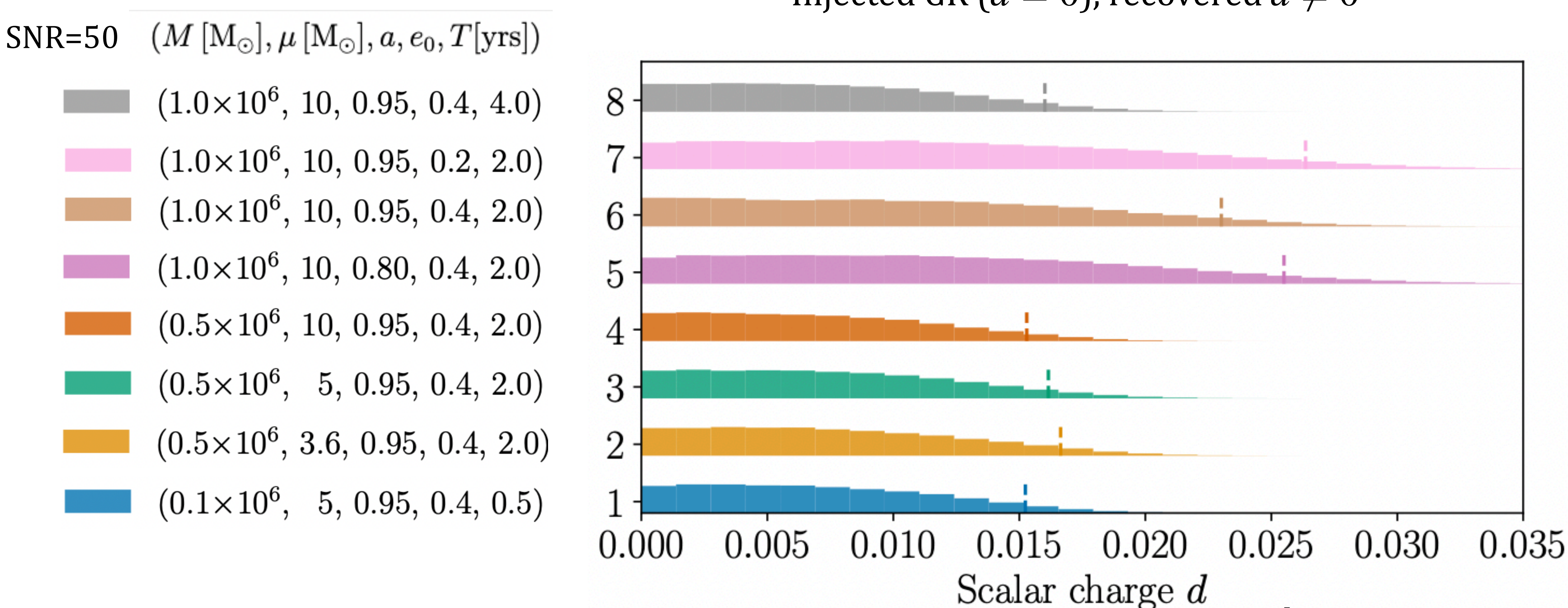

[L. Speri+, ArXiv2406.07607]

Reference System 6 vs

- System 7 (larger e_0) and System 5 (larger spin): slightly tighter bounds;
- System 4: comparable mass systems provide better bounds than more extreme mass ratios;
- System 3: fixed mass ratio but smaller secondary;
- System 8: comparing T;
- System 1: larger p_0, better bound on d;

Bayesian Analysis: Single measurement

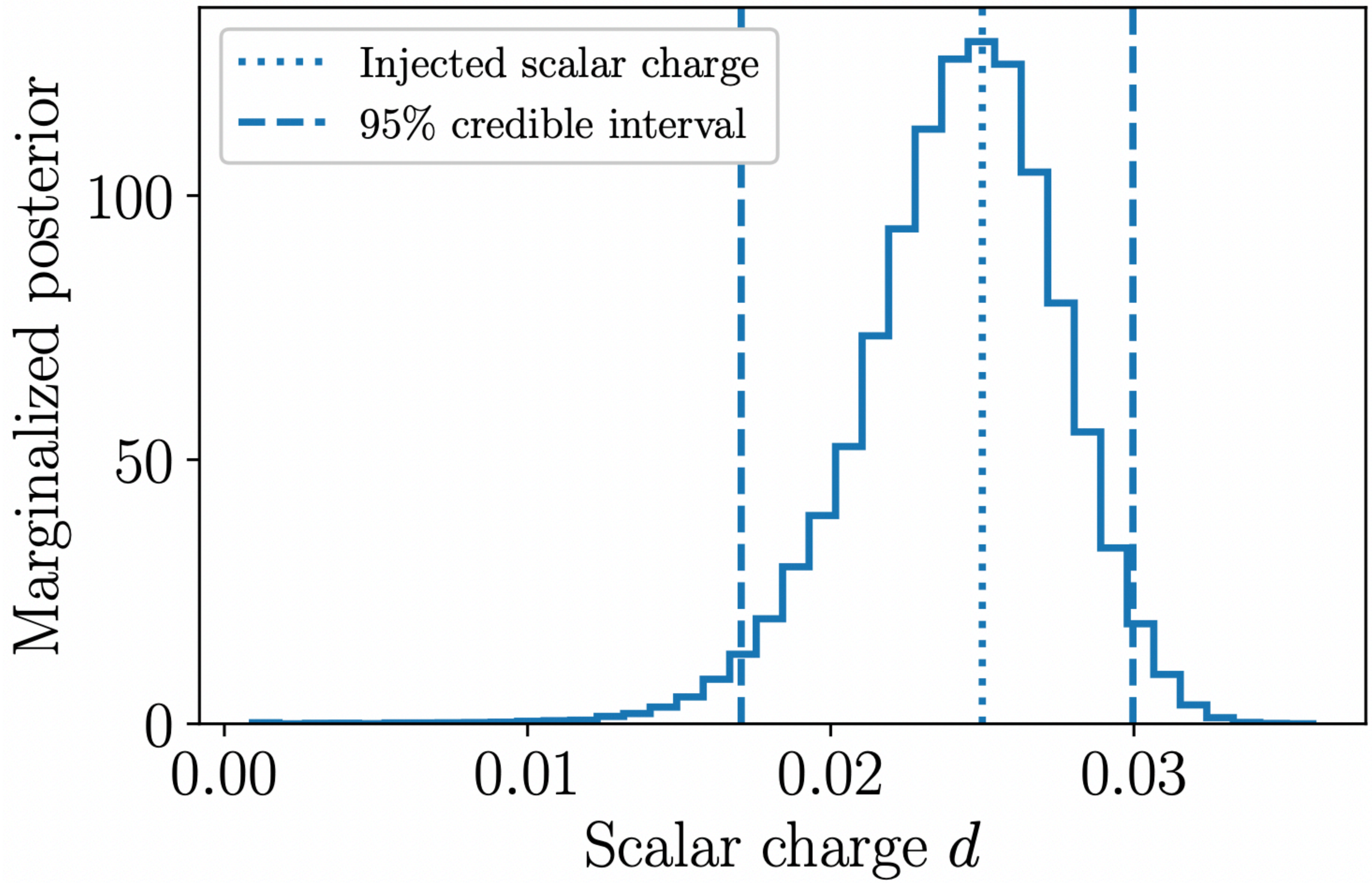

- Injected scalar charge: $d = 0.025$
- $M = 10^5 M_\odot$, $\mu = 5M_\odot$
- $T = 2$ yrs
- $SNR = 50$
- 95 % credible interval : $0.0244^{+0.006}_{-0.007}$

Bayesian Analysis: Biases

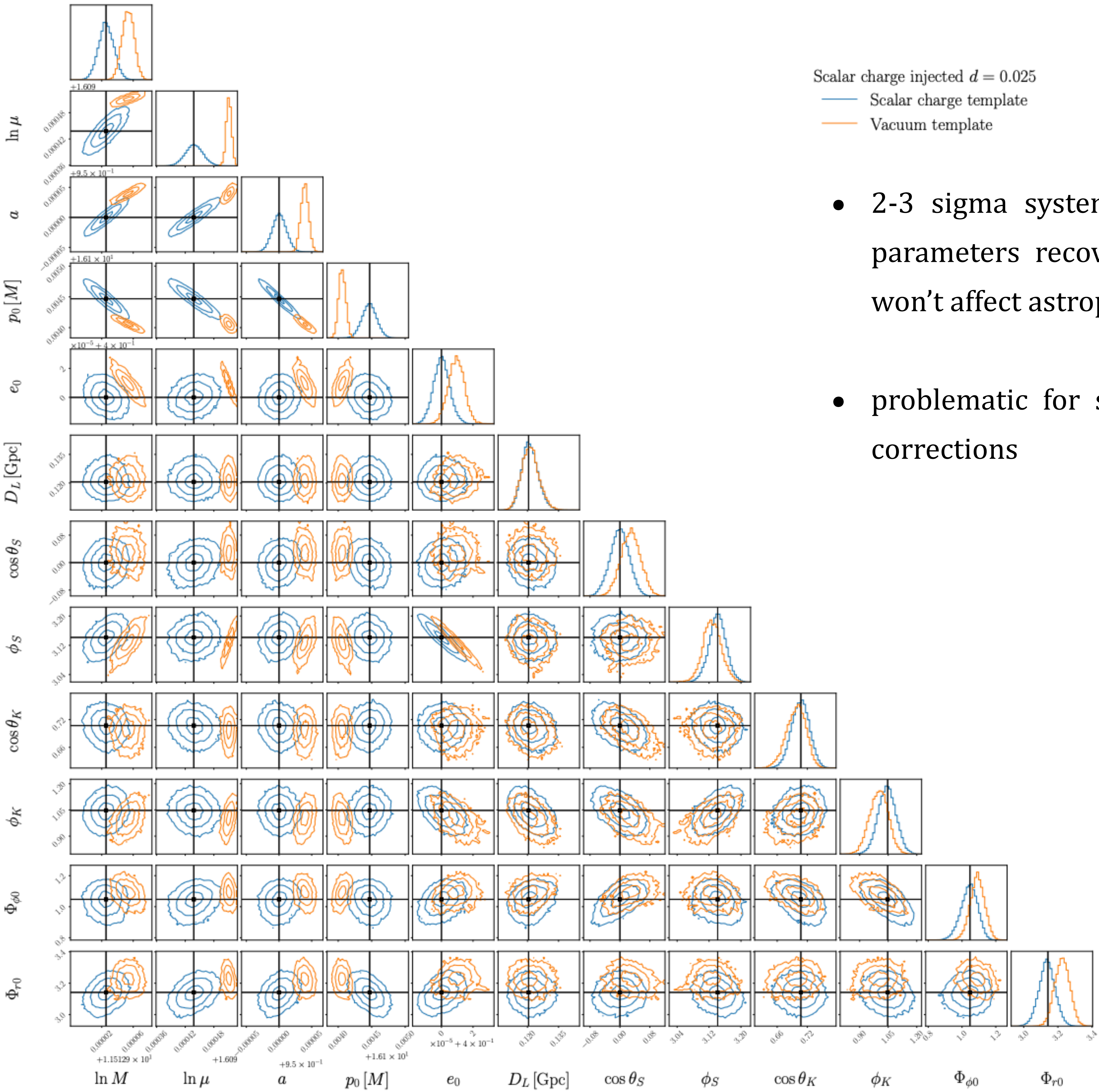

- 2-3 sigma systematic biases in the intrinsic parameters recovered with the GR template: won't affect astrophysical conclusion

- problematic for small deviations: beyond GR corrections

Bayesian Analysis: From d to α

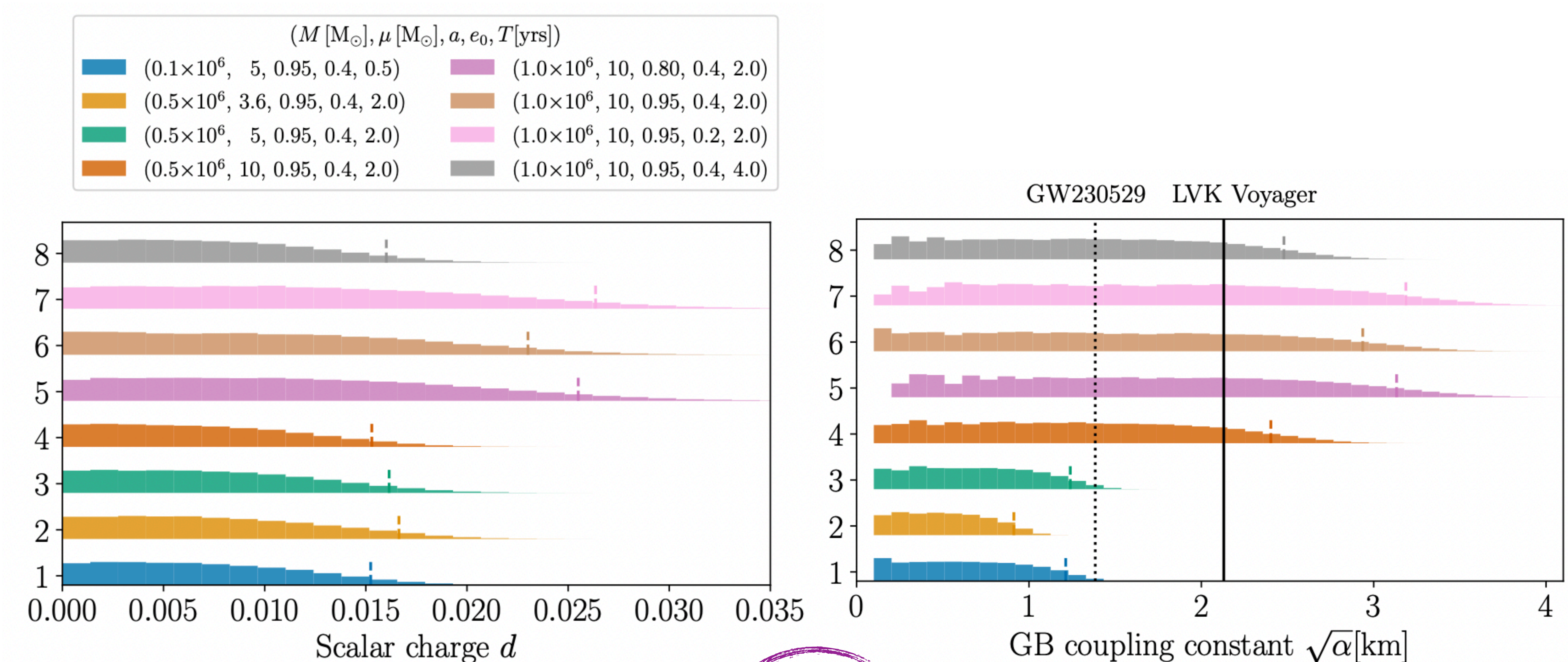

$$\alpha S_c = \frac{\alpha}{4} \int d^4x \frac{\sqrt{-g}}{16\pi} f(\varphi)\mathcal{G}$$

$$\alpha \simeq 2dm_p^2$$

$$\mathcal{G} = R^2 - 4R_{\mu\nu}R^{\mu\nu} + R_{\mu\nu\alpha\beta}R^{\mu\nu\alpha\beta}$$

$$f(\varphi) = \varphi$$

$$\alpha \simeq 2dm_p^2$$

- System 2: secondary of the same mass of the BH in GW230529 *[2406.03568]*
- Elise Sanger talk tomorrow!

EMRIs with massive scalars

Non shift-symmetric theories : the massive case

$$S = \int d^4x \frac{\sqrt{-g}}{16\pi}\left(R - \frac{1}{2}\partial_\mu\varphi\partial^\mu\varphi - \frac{1}{2}\mu_s^2\varphi^2\right) + \alpha S_c\left[\mathbf{g},\varphi\right] + S_m\left[\mathbf{g},\varphi,\Psi\right]$$

$$\left(\Box - \mu_s^2\right)\varphi = -4\pi d m_{\rm p}\int \frac{\delta^{(4)}(x - y_p(\lambda))}{\sqrt{-g}}d\lambda$$

- $\left(\frac{\mu_s M}{0.75}\right)\cdot\left(\frac{10^6 M_\odot}{M}\right)10^{-16}\ eV$
- $\bar{\mu}_s = \mu_s M$

Scalar energy emission:

- The scalar flux at infinity *vanishes* for $\omega < \mu_s$
  — For each (ℓ, m) exist r_s such that $\dot{E}^{\infty}_{scal}(r > r_s) = 0$
- The flux at the horizon is active during all the inspiral
  — Resonances for certain ω
  — Floating orbits $\dot{E}_{grav} = \dot{E}_{scal}$

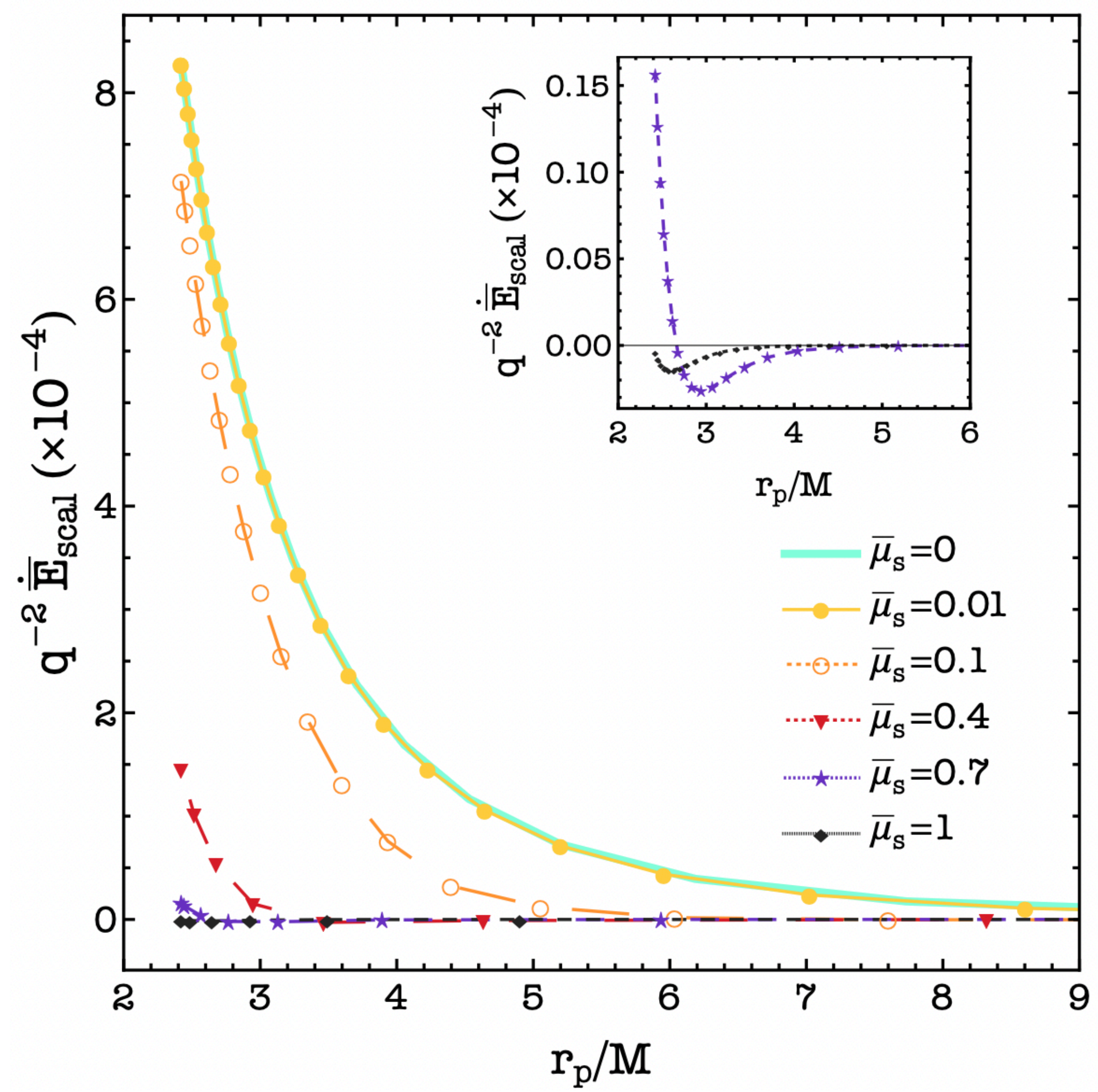

EMRIs with massive scalars: Fisher analysis

- Inject parameters to generate the waveform: $\vec{\theta} = \left(\ln M, \ln m_p, \frac{a}{M}, \ln D, \theta_S, \phi_S, \theta_L, \phi_L, r_0, \Phi_0, d, \bar{\mu}_s\right)$
- Posterior probability in the limit of large SNR: $\log p(\vec{\theta}|o) \propto \log p_0(\theta) - \frac{1}{2}\Delta_i \Gamma_{ij} \Delta_j$
- Fisher Information Matrix (FIM) analysis

$$\Gamma_{ij} = \left\langle \frac{\partial h}{\partial \theta_i} \middle| \frac{\partial h}{\partial \theta_j} \right\rangle_{\theta=\hat{\theta}} \longrightarrow \mathbf{\Sigma} = \mathbf{\Gamma}^{-1} \longrightarrow \sigma_i = \Sigma_{ii}^{1/2} \quad , \quad c_{\theta_i\theta_j} = \Sigma_{ij}^{1/2}/(\sigma_{\theta_i}\sigma_{\theta_j})$$

- We considered just the dipole for the scalar emission $(\ell = 1)$
- 1 year of observation before the plunge

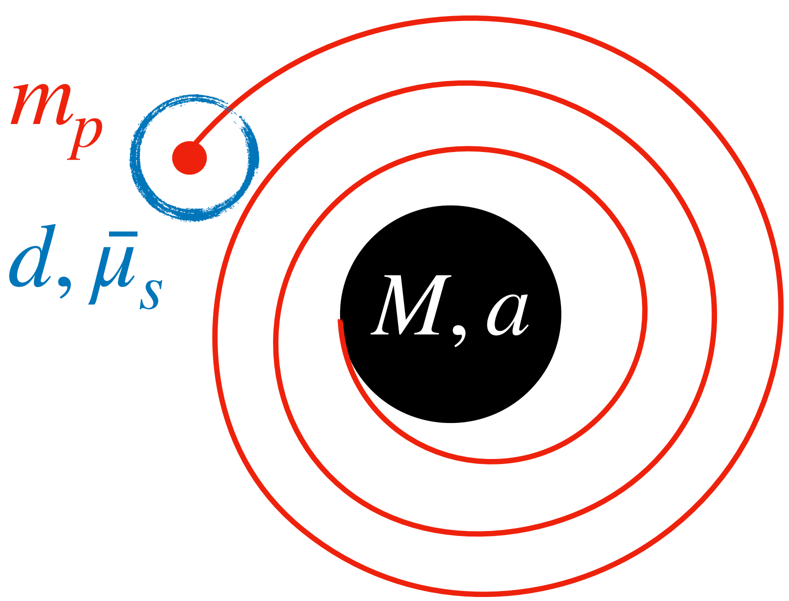

— Primary :
- $M/M_\odot = 10^6$
- $a/M = 0.9$

— Secondary :
- $m_p/M_\odot = 1.4,\ 4.6,\ 10,\ 15$
- $d = 0.1$
- $\bar{\mu}_s = 0.018,\ 0.036 \simeq 2.4,\ 4.8 \times 10^{-18} eV$

— $(\theta_S, \phi_S, \theta_L, \phi_L) = (\pi/2,\ \pi/2,\ \pi/4,\ \pi/4)$

- The scalar flux at infinity is significant throughout the entire inspiral

EMRIs with massive scalars: Fisher analysis

$m_p[M_\odot]$	$\bar{\mu}_s$	σ_d/d	$\sigma_{\bar{\mu}_s}/\bar{\mu}_s$	$c_{d\bar{\mu}_s}$
1.4	0.018	345%	2364%	0.997
	0.036	363%	391%	0.992
4.6	0.018	92%	243%	0.995
	0.036	97%	8%	−0.485
10	0.018	49%	53%	0.984
	0.036	45%	24%	−0.990
15	0.018	38%	22%	0.938
	0.036	26%	21%	−0.986

SIMULTANEOUS **detection of** ***BOTH*** **the scalar charge and mass with single event observations!**

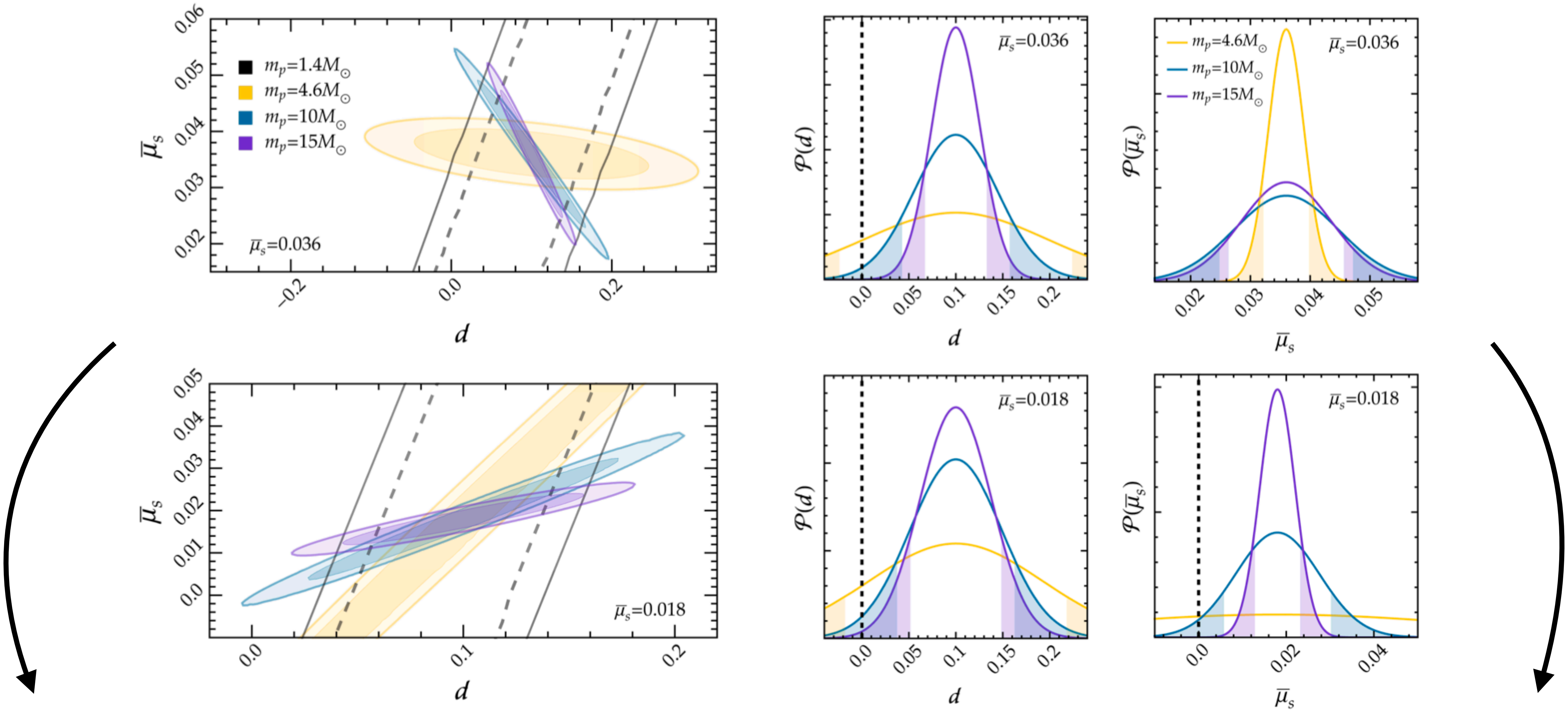

Credible intervals at 68 % and 90 % for the joint $\mathscr{P}$ of d, $\bar{\mu}_s$

White area between shaded regions: 90 % of $\mathscr{P}$

Conclusions

- EMRIs are ideal sources to test GR and search for new fundamental fields
- Theory-agnostic approach to model EMRIs in beyond-GR and beyond-SM theories with extra scalar fields
- The extra scalar energy loss affects the binary coalescence and leaves an imprint in the emitted GW
- Bayesian analysis to forecast upper bounds on the scalar charge
- For non shift-symmetric fields: fisher analysis shows how LISA could simultaneously measure both the scalar charge and mass with enough accuracy to detect new ultra-light scalar fields

TO DO:

➡ **Explore the parameter space**

➡ **Post-adiabatic corrections**

➡ **Generic orbits**

➡ **Environmental effects ..**

Work in progress !

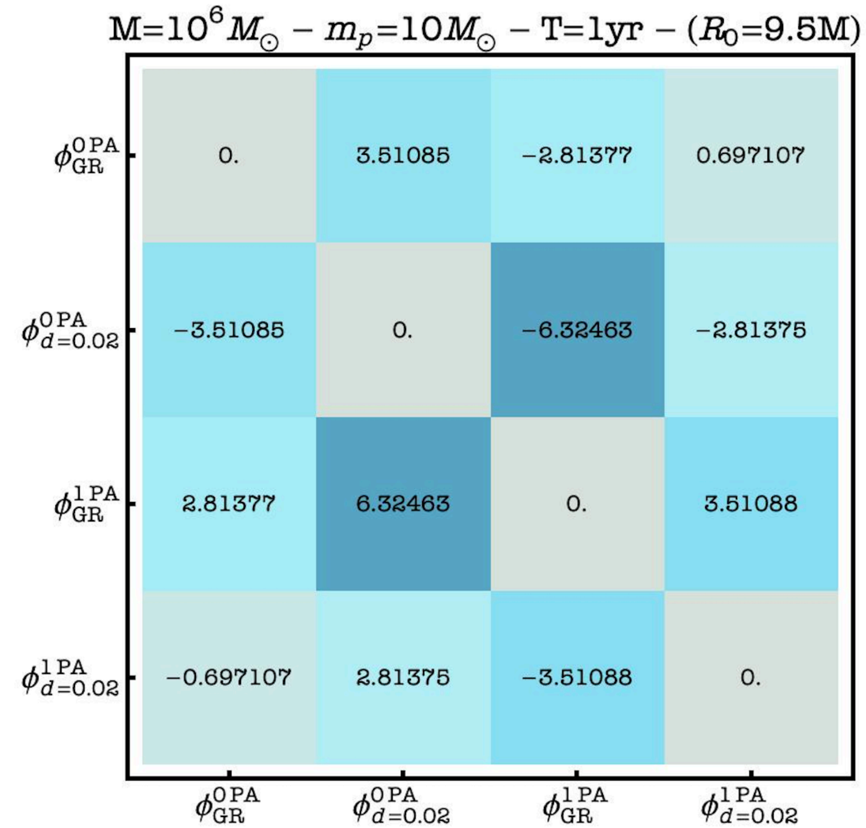

Post-Adiabatic terms

with A. Spiers, O. Burke, A.Maselli, T.Sotiriou, N. Warburton

MEW: **M**odified **E**MRI **W**aveform

With S. Gliorio, M. Della Rocca+

Thank you for the attention!

BACKUP SLIDES

Theoretical Framework

For the **secondary:** Extended body treated as a point particle

[Eardley, ApJ (1975)]

[Damour EF, PRD (1992)]

$$S_m\left[\mathbf{g},\varphi,\Psi\right] \longrightarrow S_p = -\int m\left(\varphi\right)ds = \int m\left(\varphi\right)\sqrt{g_{\mu\nu}\frac{dy_p^\mu}{d\lambda}\frac{dy_p^\nu}{d\lambda}}d\lambda$$

$m\left(\varphi\right)$: scalar function depending on the field at the location of the particle

Lenghtscales

Exterior space-time

$l \ll L$

Skeletonized body

KERR BH

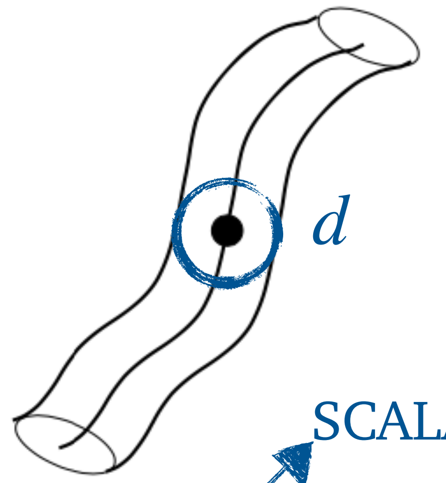

SCALAR CHARGE

- In a reference frame centered on the particle $\varphi = \varphi_0 + \frac{m_p \boxed{d}}{\tilde{r}} + O\left(\frac{m_p^2}{\tilde{r}^2}\right)$

- To evade no-hair theorems:
- Regularity conditions at Horizon

$$d = \frac{\alpha_{\mathrm{GB}}}{4\pi M}\int_{\mathcal{H}} n^a \mathcal{G}_a \, d\Omega \qquad \zeta \equiv \frac{\alpha}{(\mathbf{mass})^n}$$

Field Equations

$$S\left[\mathbf{g},\varphi,\Psi\right] = S_0\left[\mathbf{g},\varphi\right] + \alpha S_c\left[\mathbf{g},\varphi\right] + S_m\left[\mathbf{g},\varphi,\Psi\right]$$

$\boxed{\zeta \ll 1}$

$S_c \sim M^{-n} S_0$

$\dfrac{\delta S}{\delta g^{\mu\nu}}$

$$G_{\mu\nu} = \cancel{\frac{1}{2}\partial_\mu\varphi_1\partial_\nu\varphi_1 - \frac{1}{4}g_{\mu\nu}\left(\partial\varphi_1\right)^2} \quad -\frac{16\pi\alpha}{\sqrt{-g}}\cancel{\frac{\delta S_c}{\delta g^{\mu\nu}}} \sim \zeta G_{\mu\nu} \quad +8\pi\int m\left(\varphi\right)\frac{\delta^{(4)}(x-y_p(\lambda))}{\sqrt{-g}}\frac{dy_p^\alpha}{d\lambda}\frac{dy_p^\beta}{d\lambda}d\lambda$$

$\dfrac{\delta S}{\delta\varphi}$

$$\Box\varphi_1 = \quad -\frac{16\pi\alpha}{\sqrt{-g}}\cancel{\frac{\delta S_c}{\delta\varphi}} \sim \zeta\,\Box\varphi_1 \quad +16\pi\int m'\left(\varphi\right)\frac{\delta^{(4)}(x-y_p(\lambda))}{\sqrt{-g}}d\lambda$$

- m, m' to be evaluated at φ_0
- In a reference frame centered on the particle : $\varphi = \varphi_0 + \dfrac{m_p\boxed{d}}{\tilde{r}} + O\left(\dfrac{m_p^2}{\tilde{r}^2}\right)$
- Matching with the scalar field eq. outside the world tube
- (tt)-stress energy tensor in the weak field limit: matter density

$$\boxed{\begin{aligned} m'(\varphi_0) &= -\frac{d}{4}m_p \\ m(\varphi_0) &= m_p \end{aligned}}$$

Energy flux: circular orbits

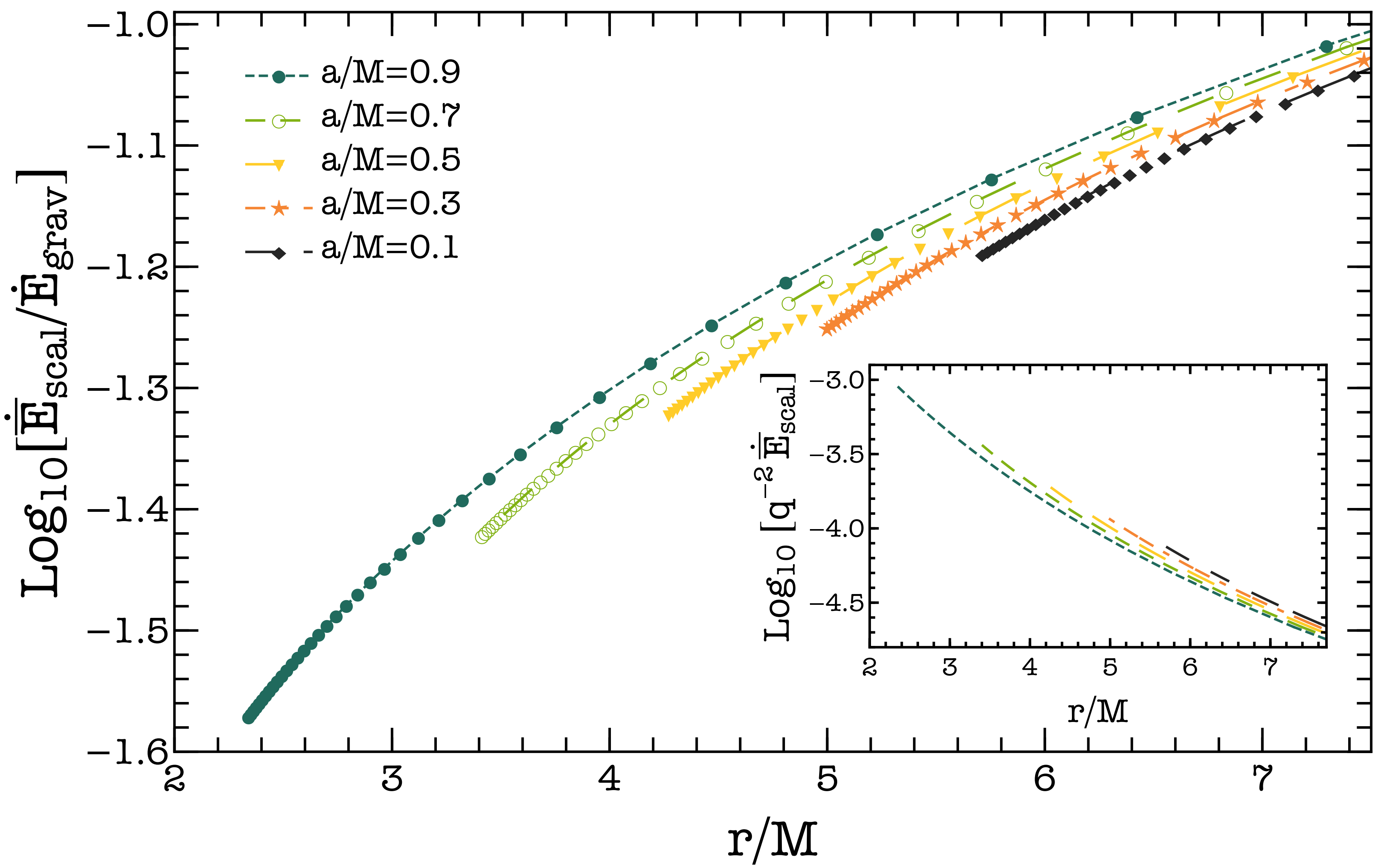

$d = 1$

- Extra energy loss in the rotating case for orbits closer to the MBH
- Increasing of the Rel. Diff. for spinning MBHs w.r.t. the non rotating ones, for a fixed R

Energy flux: eccentric orbits

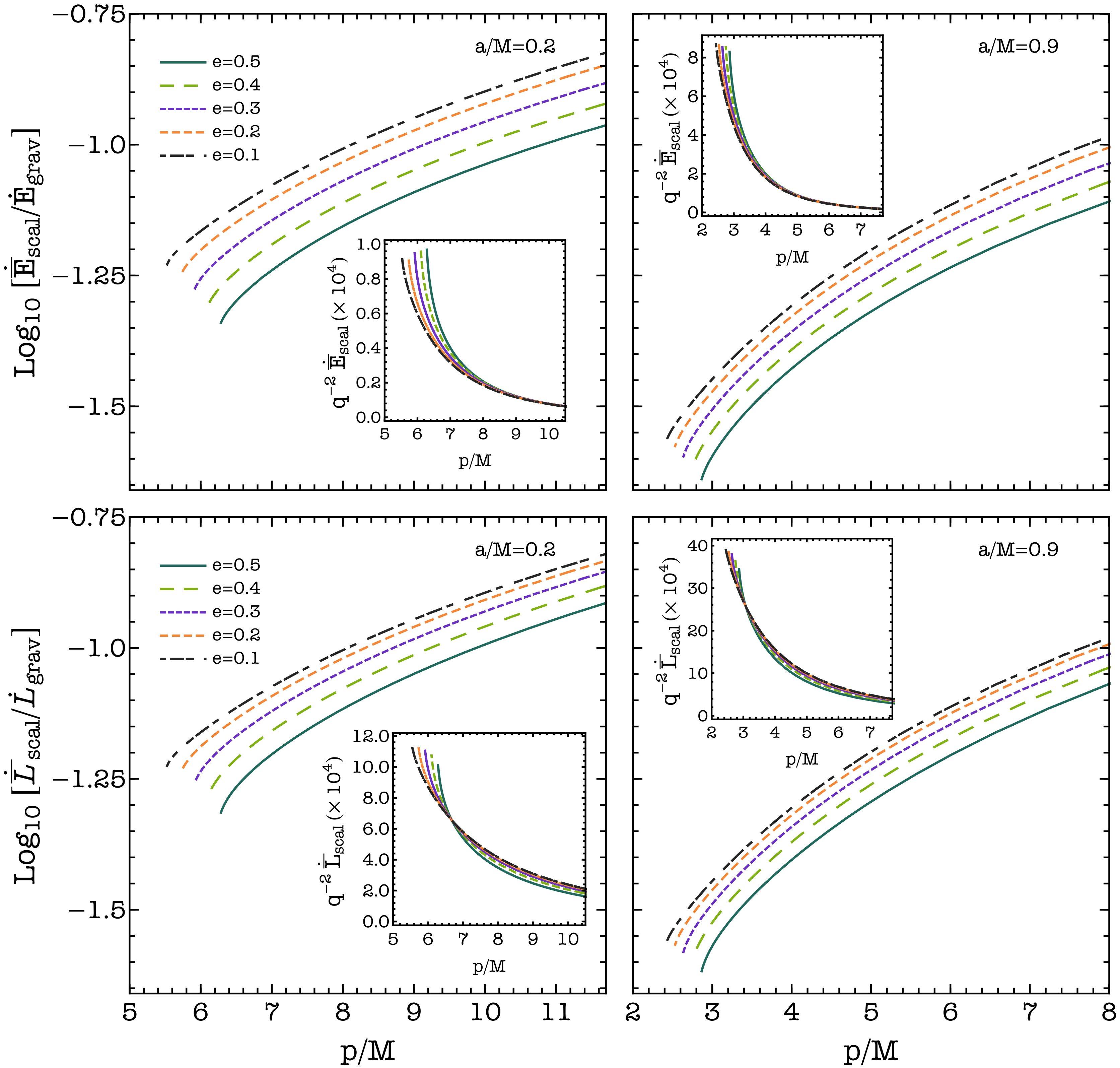

$$r(\chi) = \frac{p}{1 + e\cos\chi}$$

For a fixed e:

The Rel. Diff. decreases for smaller p, due to faster growth of $\dot{E}_{grav}$ and $\dot{L}_{grav}$w.r.t. to the scalar sector

For a fixed p:

The scalar energy flux increases with the eccentricity

The Rel. Diff. decreases with the increasing of eccentricity

Circular EMRIs: GW signal

[Barack, Cutler Phys.Rev.D 69 (2004)]

- Quadrupolar Approximation

$$h_{ij}^{TT} = \frac{2}{D}\left(P_{i\ell}P_{jm} - \frac{1}{2}P_{ij}P_{\ell m}\right)\ddot{I}_{\ell m}$$

$$I_{ij} = \int d^3x T^{tt}(t, x^i) x^i x^j = m_p x^i x^j$$

- Strain measured by the detector

$$\boxed{h(t) = \frac{\sqrt{3}}{2}\left[h_+(t)F_+(t) + h_\times(t)F_\times(t)\right]}$$

LISA pattern functions

$$F_+ = \frac{1+\cos^2\theta}{2}\cos 2\phi \cos 2\psi - \cos\theta \sin 2\phi \sin 2\psi$$

$$F_\times = \frac{1+\cos^2\theta}{2}\cos 2\phi \sin 2\psi + \cos\theta \sin 2\phi \cos 2\psi$$

Ecliptic-based system:
(θ_S, ϕ_S) *: source location*
(θ_L, ϕ_L) *: $\hat{L}$ of the secondary*

$$\cos\theta(t) = \frac{1}{2}\cos\theta_S - \frac{\sqrt{3}}{2}\sin\theta_S \cos[\phi_t - \phi_S] \, ,$$

$$\phi(t) = \alpha_0 + \phi_t + \tan^{-1}\left[\frac{\sqrt{3}\cos\theta_S + \sin\theta_S\cos[\phi_t - \phi_S]}{2\sin\theta_S \sin[\phi_t - \phi_S]}\right]$$

Amplitudes

$$h_+ = \mathscr{A}\cos[2\Phi(t) + 2\Phi_0]\left(1 + \cos^2\iota\right)$$

$$h_\times = -2\mathscr{A}\sin[2\Phi(t) + 2\Phi_0]\cos\iota$$

$$\mathscr{A} = \frac{2m_p}{D}\left[M\omega(t)\right]^{2/3}$$

Faithfulness: CIRCULAR EMRIs

Estimate of how much two signals differ: $\mathcal{F}[h_1, h_2] = \max_{\{t_c, \phi_c\}} \frac{\langle h_1 | h_2 \rangle}{\sqrt{\langle h_1 | h_1 \rangle \langle h_2 | h_2 \rangle}}$

Inner product $\langle h_1 | h_2 \rangle = 4\Re \int_{f_{min}}^{f_{\max}} \frac{\tilde{h}_1(f)\tilde{h}_2^\star(f)}{S_n(f)} df$

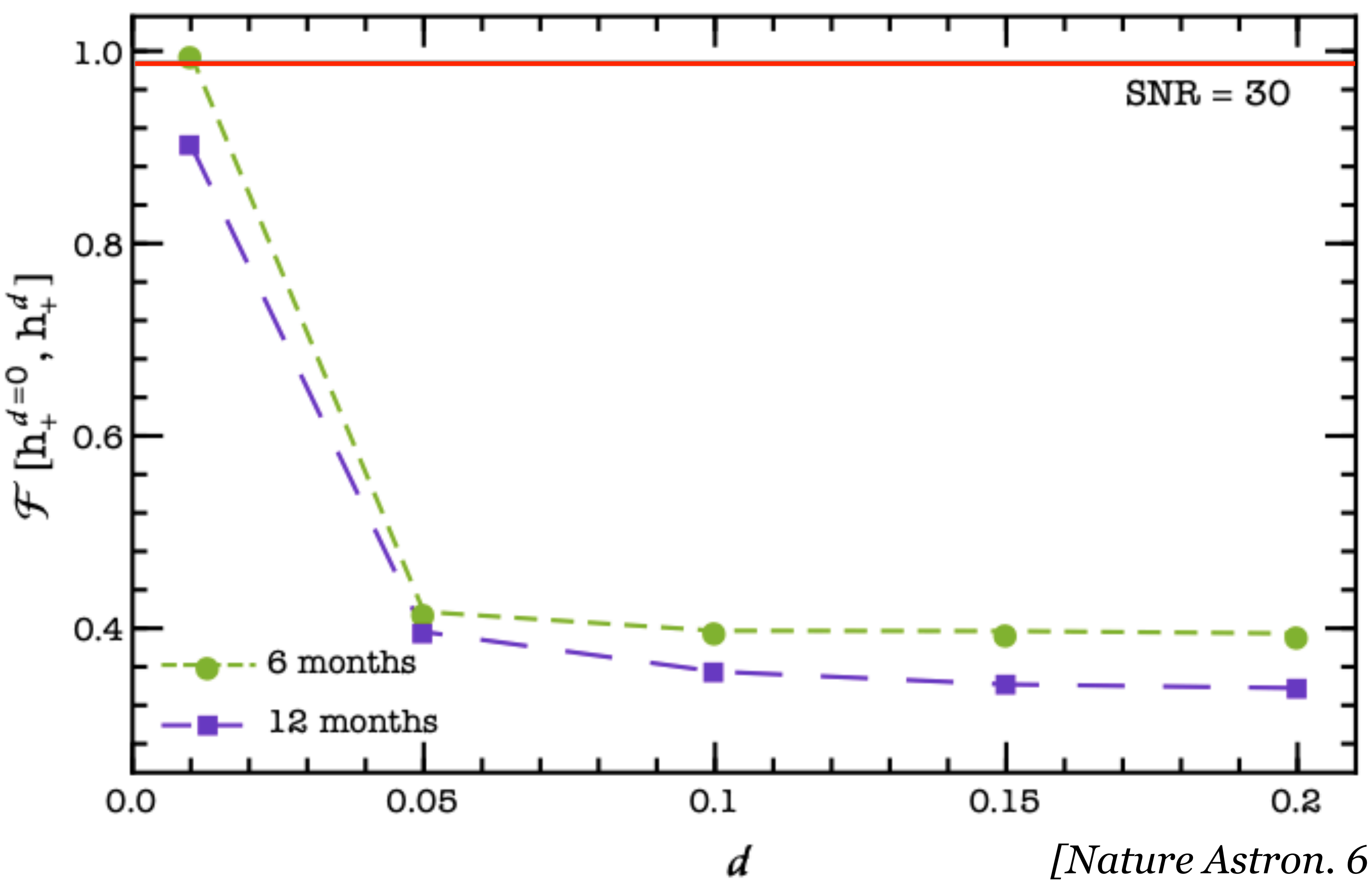

detectable effect !

[Nature Astron. 6 (2022) 4, 464-470]

- Red line: threshold under which the signals are significantly different - $\mathcal{F} \lesssim 0.988$ for $SNR = 30$
- After 1year $\mathcal{F}$ is always smaller than the threshold for scalar charges as small as $d = 0.05$

Circular EMRIs: Fisher Information Matrix

- Inject parameters to generate the waveform $\vec{\theta} = \left(\ln M, \ln m_p, a/M, \ln D, \theta_S, \phi_S, \theta_L, \phi_L, r_0, \Phi_0, d \right)$
- Fisher Information Matrix analysis

- Results for $M = 10^6 M_\odot$, $a/M = 0.9$, $m_p = 10 M_\odot$ (CIRCULAR INSPIRAL)

LISA potentially able to measure scalar charges with % error !

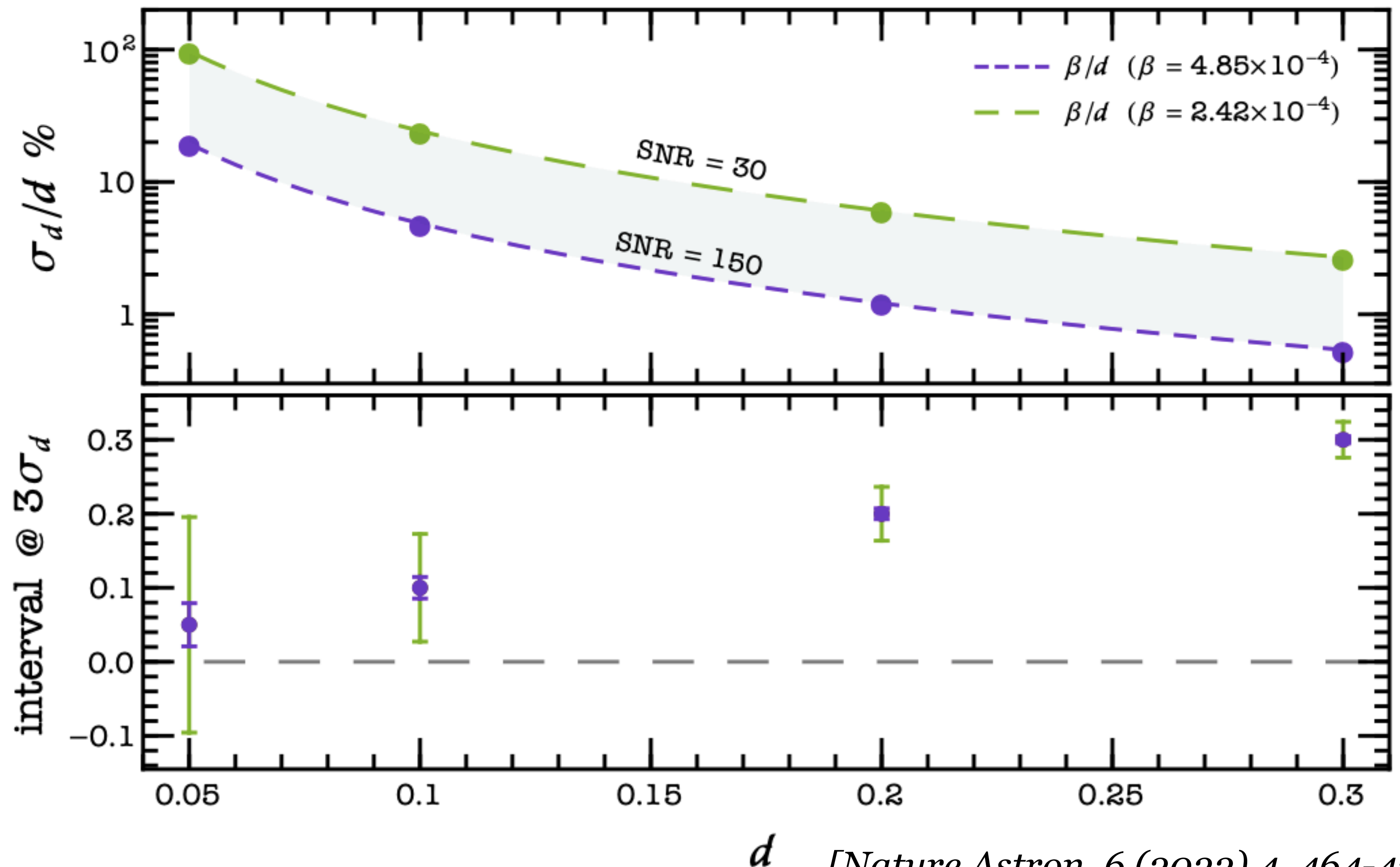

[Nature Astron. 6 (2022) 4, 464-470]

EMRIs with massive scalars: Faithfulness

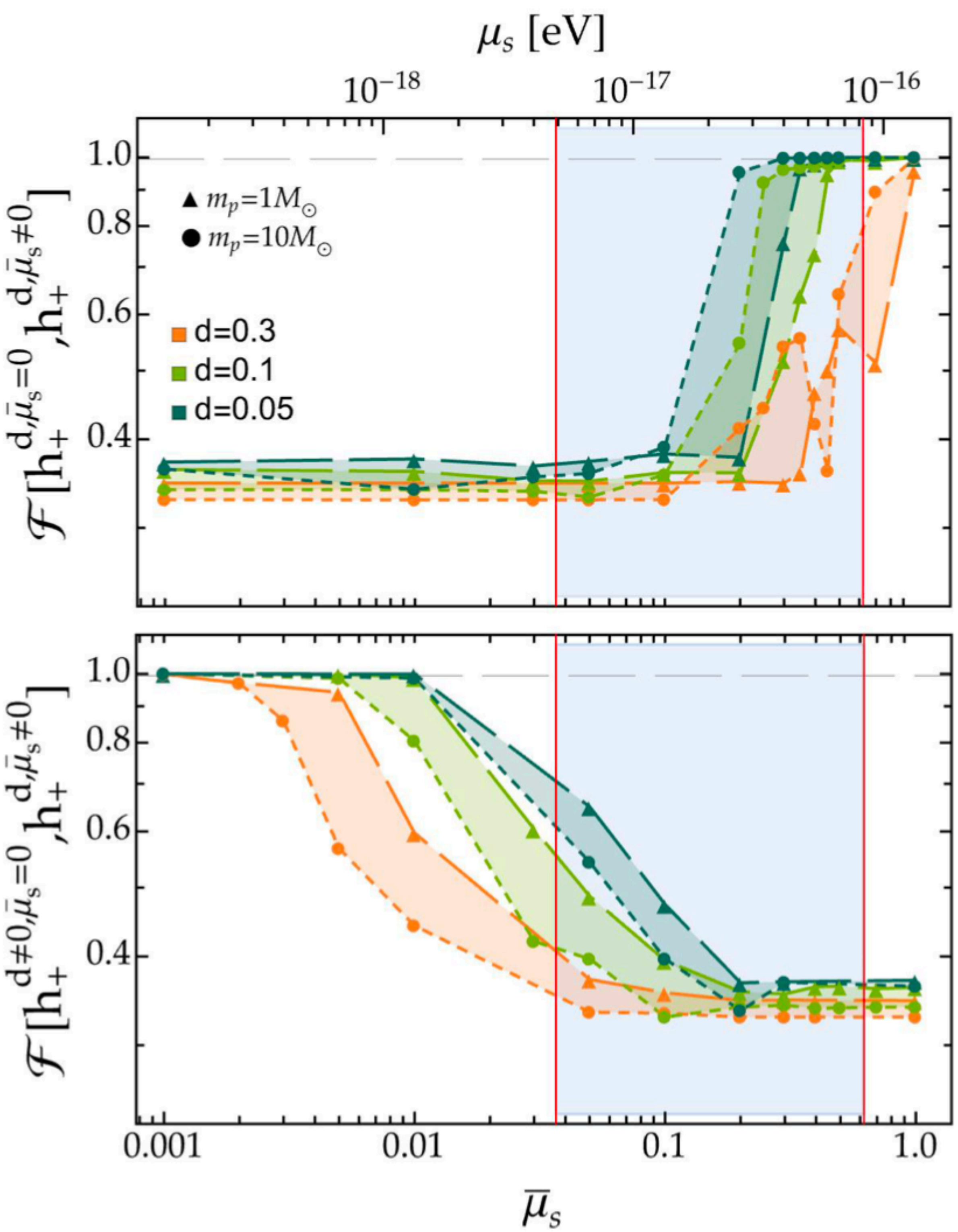

[Phys.Rev.Lett. 131 (2023) 5]

- Upper panel: GR vs massive case
- Lower panel: massless vs massive case
- Detectability threshold $\mathcal{F} \lesssim 0.994$ for $SNR = 30$
- Shaded band: superradiance instability
  - $a/M = 0.9$ [Brito+, Lect.Notes Phys. 971 (2020) pp.1-293]
  - $M = 10^6 M_\odot$
- Large $\bar{\mu}_s$: suppression of the energy flux at infinity
- Small $\bar{\mu}_s$: massive case undistinguishable from the massless case

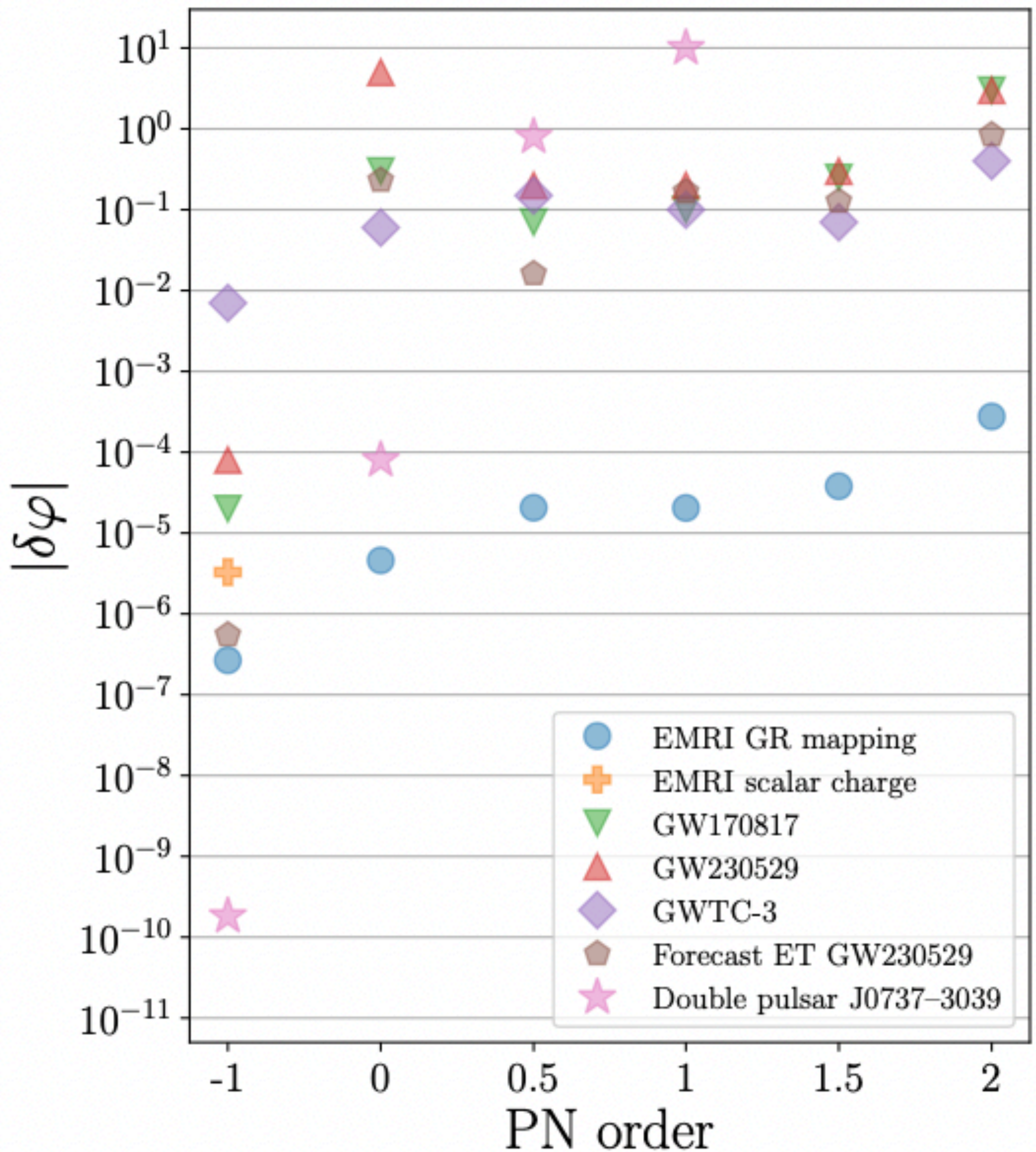

10^{1}
10^{0}
10^{-1}
10^{-2}
10^{-3}
10^{-4}
10^{-5}
10^{-6}
10^{-7}
10^{-8}
10^{-9}
10^{-10}
10^{-11}
$|\delta\varphi|$
-1
0
0.5
1
1.5
2
PN order
EMRI GR mapping
EMRI scalar charge
GW170817
GW230529
GWTC-3
Forecast ET GW230529
Double pulsar J0737–3039

Orbital Evolution

The emitted GW flux drives the adiabatic orbital evolution

- Balance law $\dot{E} = -\dot{E}_{GW}$ $\quad$ $\dot{L} = -\dot{L}_{GW}$

- From the rate of change of the integrals (E, L), we obtain the time derivatives of (p, e)

$$\dot{p} = (L_{,e}\dot{E} - E_{,e}\dot{L})/H$$

$$H = E_{,p}L_{,e} - E_{,e}L_{,p}$$

$$\dot{e} = (E_{,p}\dot{L} - L_{,p}\dot{E})/H$$

- And of the phases $\psi_{\phi,r}$ related to the frequencies $\boxed{\Omega_{\phi,r}(e,p) = \frac{d}{dt}\Psi_{\phi,r}}$

- The extra emission accelerates the binary coalescence and affects the GW phase, causing a **dephasing** w.r.t the case $d = 0$

- Compute the dephasing

$$\boxed{\Delta\Psi_i = 2\int_0^{T_{obs}} \Delta\Omega_i dt \qquad i = \phi, r}$$

$$\Delta\Omega_i = \Omega_i^d - \Omega_i^{d=0}$$

GW Signal

- Quadrupolar approximation $$h_{ij}^{TT} = \frac{2}{D}\left(P_{i\ell}P_{jm} - \frac{1}{2}P_{ij}P_{\ell m}\right)\ddot{I}_{\ell m}$$

[L. Barack and C. Cutler, Phys. Rev. D 69 (2004) 082005]

$$I_{ij} = \int d^3x T^{tt}(t, x^i)x^i x^j = m_p x^i x^j$$

- Strain measured by the detector $$h(t) = \sum_n h_n(t) \qquad h_n(t) = \frac{\sqrt{3}}{2}\left[F^+(t)A_n^+(t) + F^\times(t)A_n^\times(t)\right]$$

LISA pattern functions

$$F_+ = \frac{1+\cos^2\theta}{2}\cos 2\phi \cos 2\psi - \cos\theta \sin 2\phi \sin 2\psi$$
$$F_\times = \frac{1+\cos^2\theta}{2}\cos 2\phi \sin 2\psi + \cos\theta \sin 2\phi \cos 2\psi$$

Amplitudes

$$A_n^+ = -[1 + (\hat{L}\cdot\hat{N})^2][a_n \cos(2\gamma) - b_n \sin(2\gamma)] + [1 - (\hat{L}\cdot\hat{N})^2]c_n$$
$$A_n^\times = 2(\hat{L}\cdot\hat{N})[b_n \cos(2\gamma) + a_n \sin(2\gamma)]$$

$$a_n = -n\boxed{\mathcal{A}}\left[J_{n-2}(ne) - 2eJ_{n-1}(ne) + (2/n)J_n(ne) + 2eJ_{n+1}(ne) - J_{n+2}(ne)\right]\cos[n\Phi(t)]$$

$$b_n = -n\boxed{\mathcal{A}}(1-e^2)^{1/2}[J_{n-2}(ne) - 2J_n(ne) + J_{n+2}(ne)]\sin[n\Phi(t)]$$

$$c_n = 2\boxed{\mathcal{A}}J_n(ne)\ \cos[n\Phi(t)]$$

$$(2\pi\nu M)^{2/3}m_p/D$$

$$\begin{cases} 2\pi\nu = d\Phi/dt \\ \Phi = \Psi_\phi \\ \cos\gamma = \cos\Psi_R \end{cases}$$

Dephasing: circular orbits

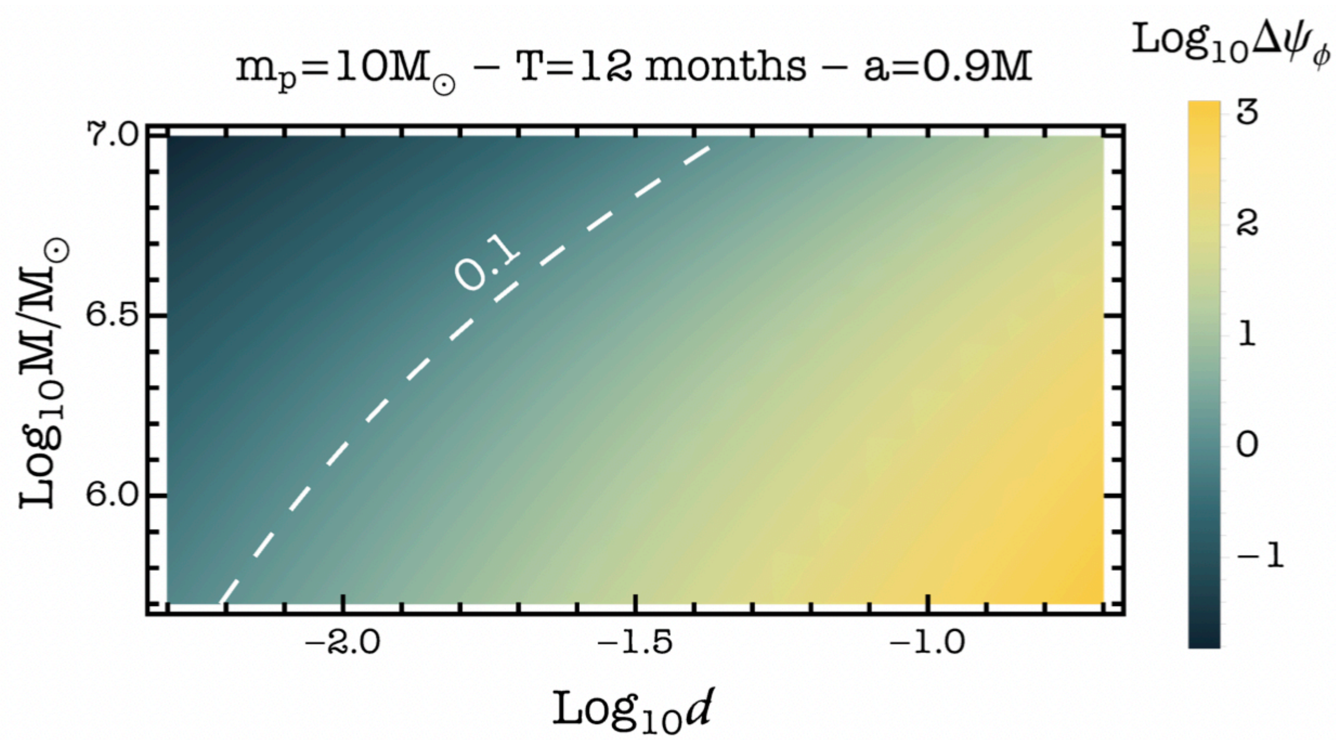

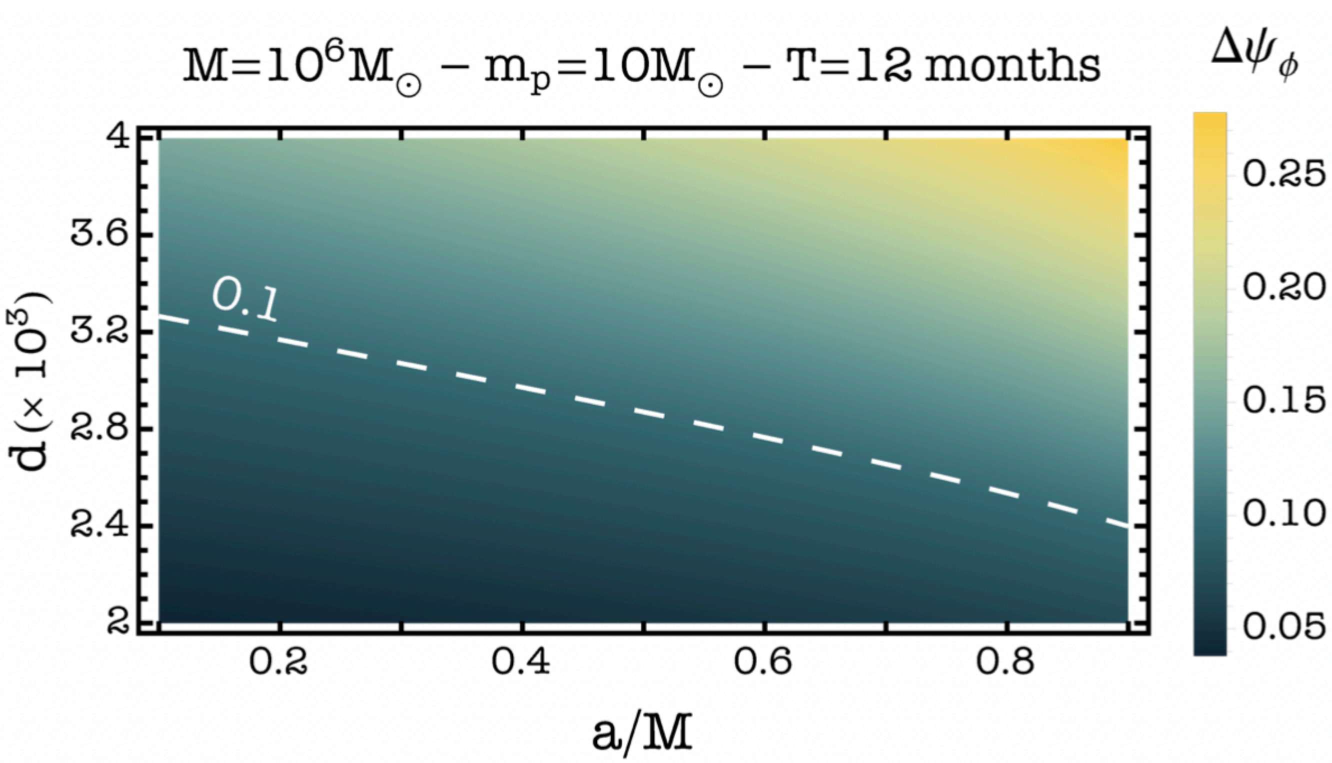

- White dashed line: threshold of phase resolution by LISA of $\boxed{\Delta\psi_\phi = 0.1 \text{ for } SNR = 30}$
- $\Delta\psi_\phi$ significant: for $M \lesssim 10^6 M_\odot$ it can be larger than 10^3 radians
- $\Delta\psi_\phi$ increases with the spin of the primary

Dephasing: inclined circular orbits

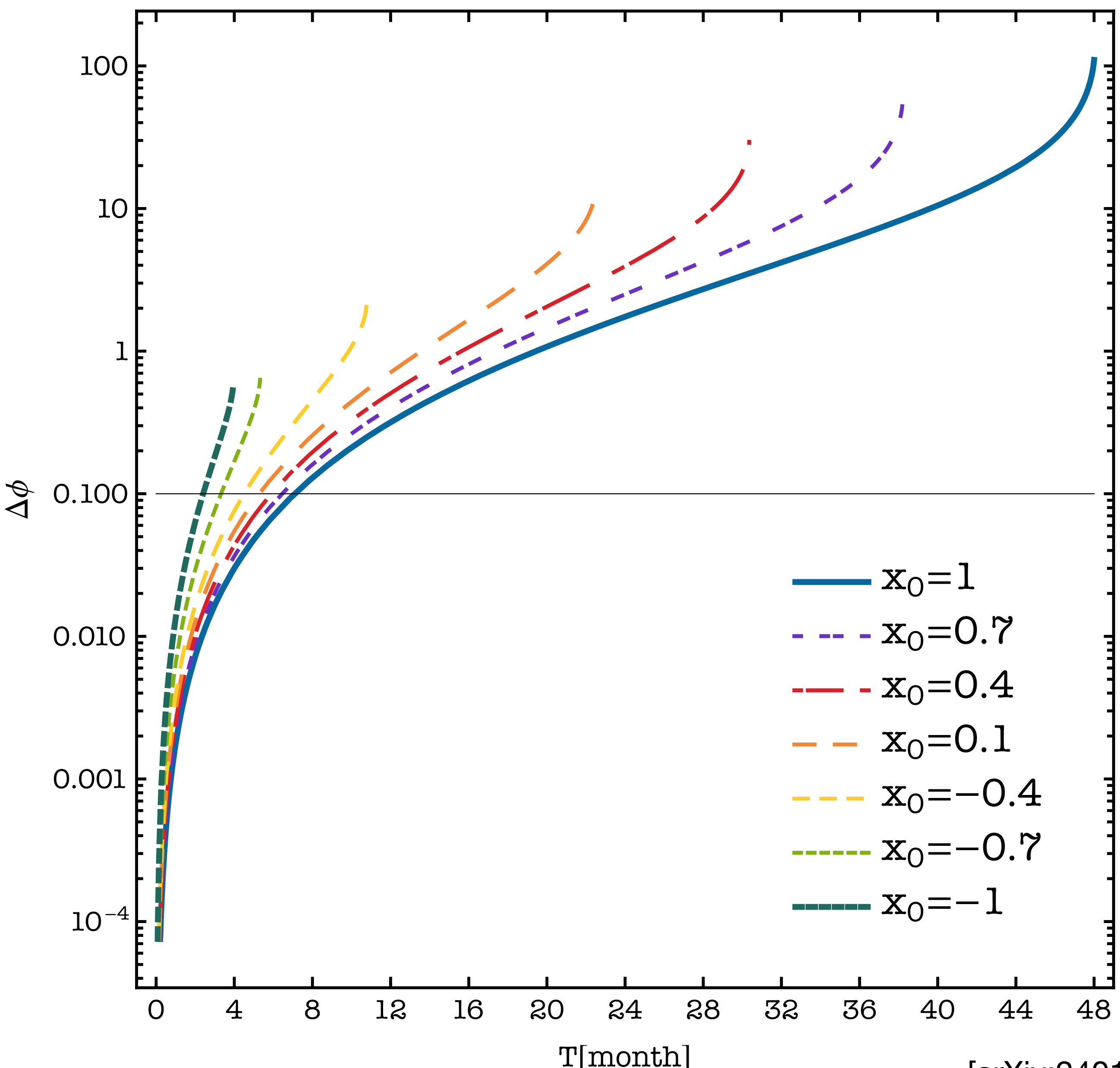

[arXiv:2401.09542]

- $M = 10^6 M_\odot$
  $m_p = 10\ M_\odot$
  $a = 0.95M$
- $r_0 = 10M$
  $d = 0.01$

$$\theta_{min} \leq \theta \leq \pi - \theta_{min}$$

$$\theta_{\rm inc} + (\operatorname{sgn} L_z)\theta_{\rm min} = \frac{\pi}{2}$$

$$x = \cos\theta_{inc}$$

- Increasing x_0, the time it takes for the secondary to reach the plunge grows, leading to larger accumulated dephasings
- For a given time of observation, $\Delta\Psi_\phi$ is larger for inspirals with higher x_0
- After 3-4 months all the inspirals lead to a dephasing larger then the threshold !

Circular EMRIs: Fisher Information Matrix

For hairy BHs, if the little body is a BH, we find a relation $d(\alpha)$

[Nature Astron. 6 (2022) 4, 464-470]

Shift-symmetric Gauss Bonnet gravity:

$$\alpha S_c = \frac{\alpha}{4}\int d^4x \frac{\sqrt{-g}}{16\pi} f(\varphi)\mathscr{G}$$

$$\mathscr{G} = R^2 - 4R_{\mu\nu}R^{\mu\nu} + R_{\mu\nu\alpha\beta}R^{\mu\nu\alpha\beta}$$

$$f(\varphi) = \varphi$$

$$\alpha \simeq 2dm_p^2 - \frac{73}{240}d^3m_p^2$$

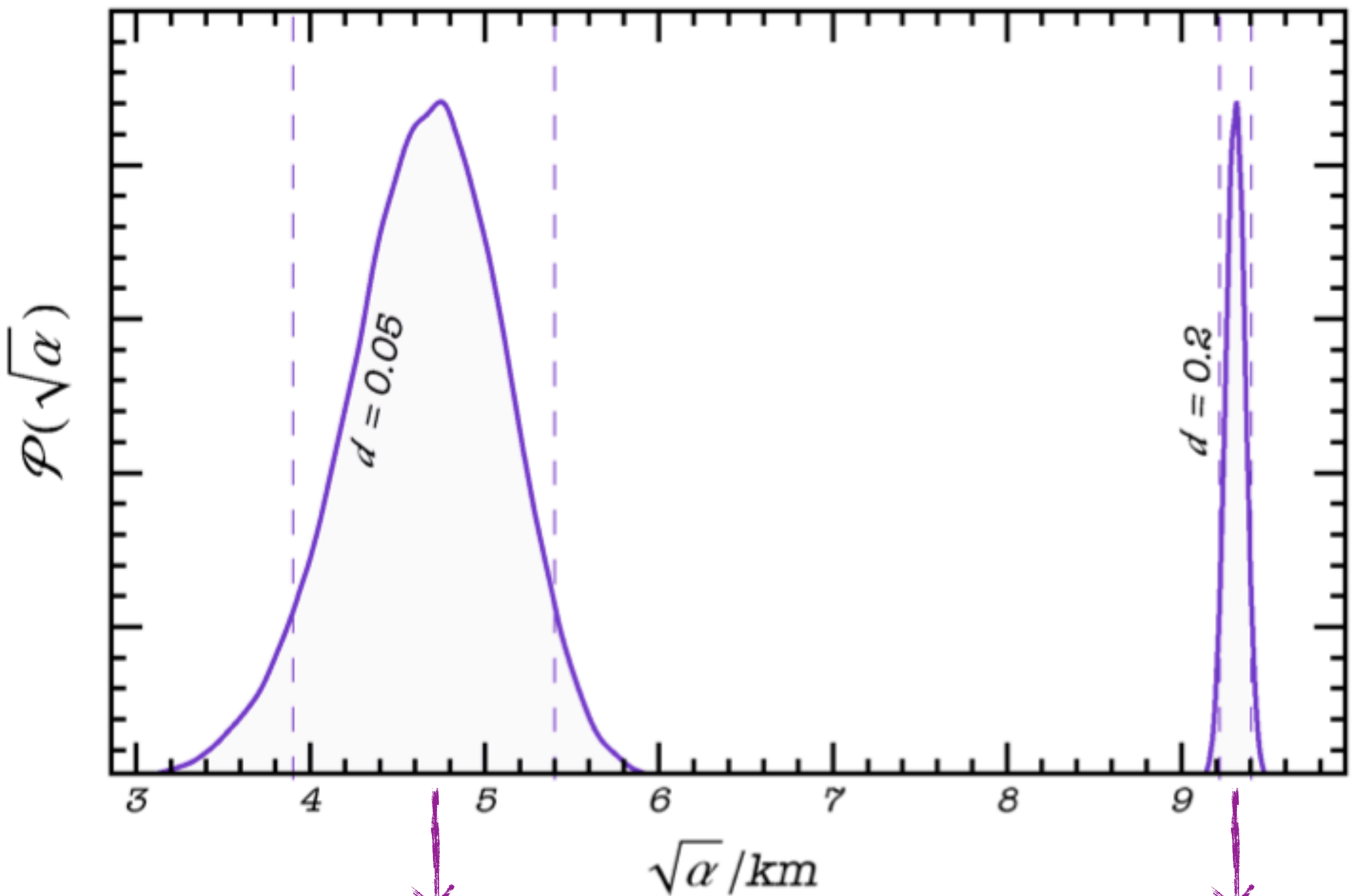

$\sqrt{\alpha}/km = 4.67^{+0.73}_{-0.77}$ $\sqrt{\alpha}/km = 9.312^{+0.092}_{-0.092}$

- Probability density function of $\sqrt{\alpha}$ from the joint probability distribution of m_p and d (SNR=150)
- Vertical lines: 90 % confidence interval

Eccentric equatorial EMRIs

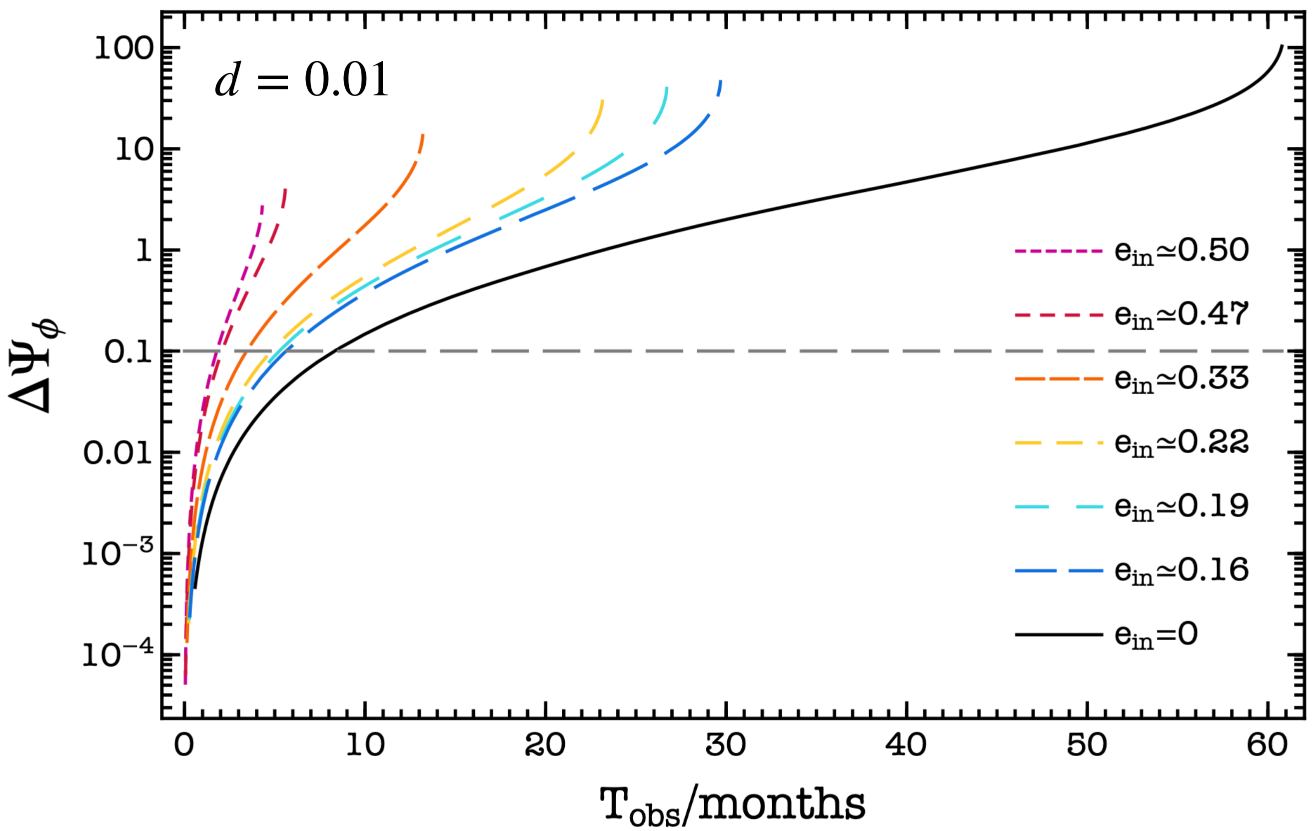

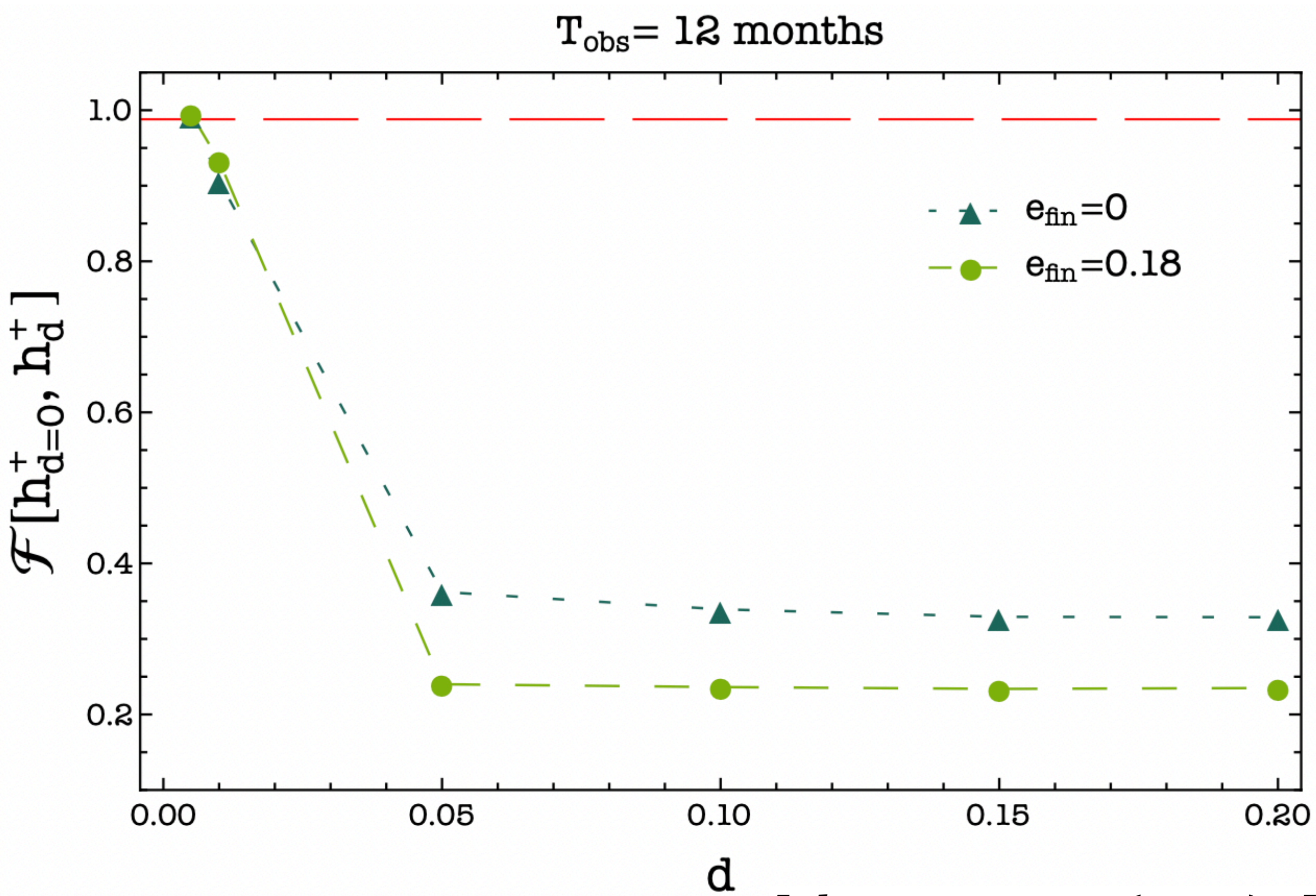

[Phys.Rev.D 106 (2022) 4]

- $r(\chi) = \dfrac{p}{1 + e\cos\chi}$
- after 3-4 months all the inspirals lead to a dephasing larger then the threshold !
- for a given time of observation, $\Delta\Psi_\phi$ is larger for inspirals with higher e_{in}

- Red line: threshold under which the signals are significantly different - $\boxed{\mathcal{F} \lesssim 0.994 \text{ for } SNR = 30}$
- After 1year $\mathcal{F}$ is always smaller than the threshold for scalar charges as small as $d = 0.01$
- For the eccentric inspirals the distinguishability increases

Orbital Evolution

The emitted GW flux drives the adiabatic orbital evolution

- Balance law $\dot{E} = -\dot{E}_{GW}$
- Time evolution of the coordinates $\big(r(t), \Phi(t)\big)$: $\dot{r} = -\dot{E}\dfrac{dr}{dE_{\rm orb}}\,, \quad \dot{\Phi} = \Omega_p = \dfrac{M^{1/2}}{r^{3/2} + \chi M^{3/2}}$
- Dephasing $\Delta\phi = 2\int_0^{T_{obs}} [\Omega_{d,\bar{\mu}_s=0} - \Omega_{d,\bar{\mu}_s\neq 0}]\, dt$

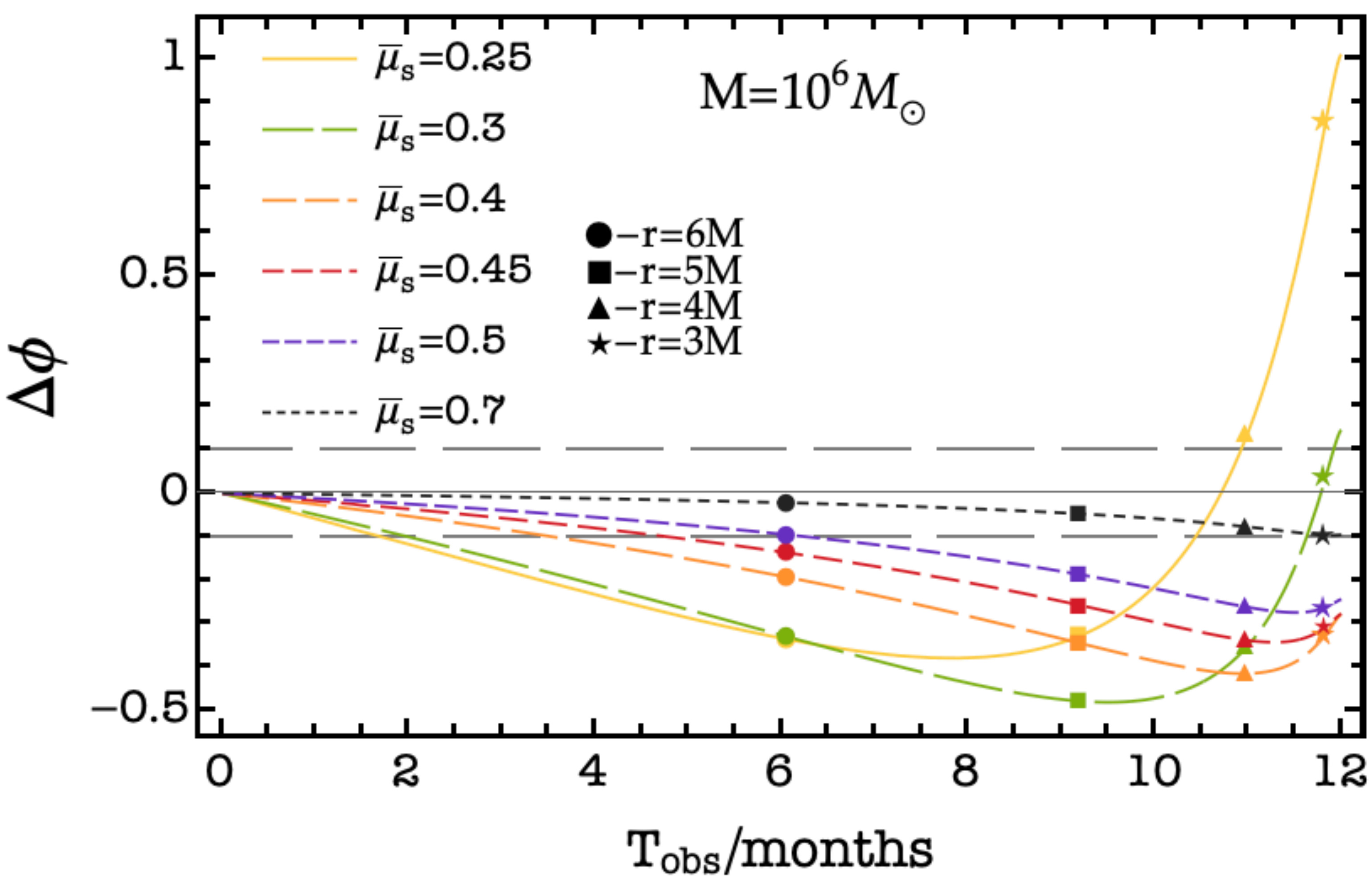

- $\chi = 0.9$
- $m_p = 10 M_\odot$
- $d = 0.1$

- Horizontal lines: threshold of phase resolution by LISA of $\Delta\psi_\phi = \pm 0.1$ for $SNR = 30$

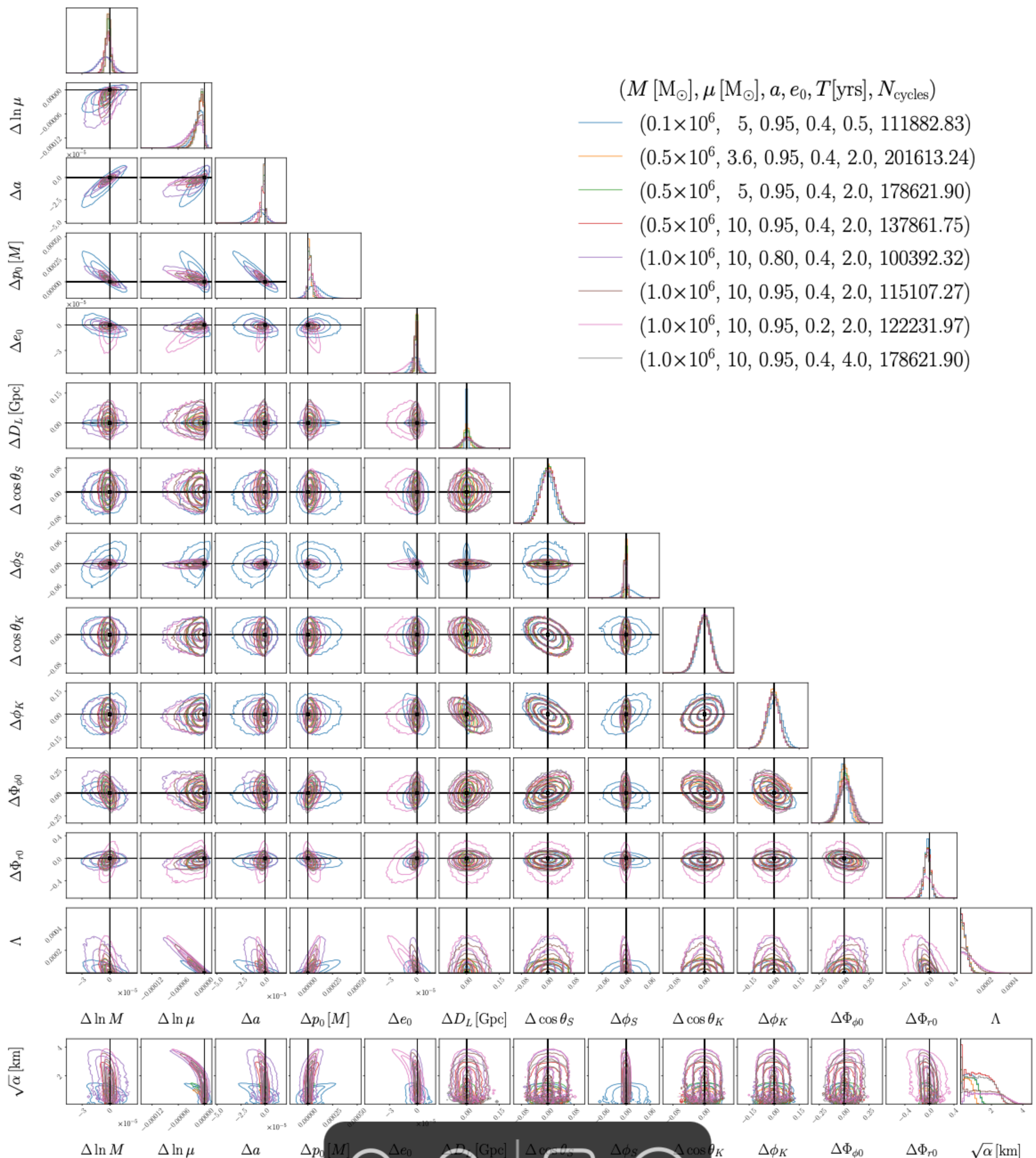

$(M\,[\mathrm{M}_\odot], \mu\,[\mathrm{M}_\odot], a, e_0, T[\mathrm{yrs}], N_{\mathrm{cycles}})$
$(0.1\times10^6,\ 5,\ 0.95,\ 0.4,\ 0.5,\ 111882.83)$
$(0.5\times10^6,\ 3.6,\ 0.95,\ 0.4,\ 2.0,\ 201613.24)$
$(0.5\times10^6,\ 5,\ 0.95,\ 0.4,\ 2.0,\ 178621.90)$
$(0.5\times10^6,\ 10,\ 0.95,\ 0.4,\ 2.0,\ 137861.75)$
$(1.0\times10^6,\ 10,\ 0.80,\ 0.4,\ 2.0,\ 100392.32)$
$(1.0\times10^6,\ 10,\ 0.95,\ 0.4,\ 2.0,\ 115107.27)$
$(1.0\times10^6,\ 10,\ 0.95,\ 0.2,\ 2.0,\ 122231.97)$
$(1.0\times10^6,\ 10,\ 0.95,\ 0.4,\ 4.0,\ 178621.90)$
$\Delta\ln\mu$
Δa
$\Delta p_0\,[M]$
Δe_0
$\Delta D_L\,[\mathrm{Gpc}]$
$\Delta\cos\theta_S$
$\Delta\phi_S$
$\Delta\cos\theta_K$
$\Delta\phi_K$
$\Delta\Phi_{\phi0}$
$\Delta\Phi_{r0}$
Λ
$\Delta\ln M$
$\sqrt{\alpha}\,[\mathrm{km}]$